

# 1 **Evolutionary origin of sex differentiation system in insects**

2

3 Yasuhiko Chikami<sup>1,2</sup>, Miki Okuno<sup>3</sup>, Atsushi Toyoda<sup>4,5</sup>, Takehiko Itoh<sup>6</sup>, Teruyuki

4 Niimi<sup>1,2\*</sup>

5

6 <sup>1</sup>Division of Evolutionary Developmental Biology, National Institute for Basic

7 Biology, 38 Nishigonaka, Myodaiji, Okazaki, Aichi, 444-8585, Japan

8 <sup>2</sup>Department of Basic Biology, School of Life Science, The Graduate University for

9 Advanced Studies, SOKENDAI, 38 Nishigonaka, Myodaiji, Okazaki, Aichi, 444-

10 8585, Japan

11 <sup>3</sup>Division of Microbiology, Department of Infectious Medicine, Kurume University

12 School of Medicine, 67 Asahi-machi, Kurume, Fukuoka, 830-0011, Japan

13 <sup>4</sup>Comparative Genomics Laboratory, National Institute of Genetics, 1111 Yata,

14 Mishima, Shizuoka 411-8540, Japan

15 <sup>5</sup>Advanced Genomics Center, National Institute of Genetics, 1111 Yata, Mishima,

16 Shizuoka 411-8540, Japan

17 <sup>6</sup>School of Life Science and Technology, Tokyo Institute of Technology, 2-12-1

18 Ookayama, Meguro, Tokyo, 152-8550, Japan

19 **\*Corresponding author:**

20 Teruyuki Niimi

21 E-mail: [niimi@nibb.ac.jp](mailto:niimi@nibb.ac.jp)

22 **This PDF file includes:**

23 Main Text

24 Figures 1 to 6

25

## 26 **Abstract**

27 The evolution of the functionality of genes and genetic systems is a major source of  
28 animal diversity. Its best example is insect sex differentiation systems: promoting  
29 male and female differentiation (dual-functionality) or only male differentiation  
30 (single-functionality). However, the evolutionary origin of such functional diversity is  
31 largely unknown. Here, we investigate the ancestral functions of *doublesex*, a key  
32 factor of insect sex differentiation system, using the apterygote insect, *Thermobia*  
33 *domestica*, and reveal that its *doublesex* is essential for only males at the phenotypic  
34 level, but contributes to promoting female-specific *vitellogenin* expression in females.  
35 This functional discordance between the phenotypic and transcription-regulatory  
36 levels in *T. domestica* shows a new type of functionality of animal sex differentiation  
37 systems. Then, we examine how the sex differentiation system transited from the  
38 single-functionality to the dual-functionality in phenotypes and uncover that a  
39 conserved female-specific motif of *doublesex* is detected in taxa with the dual-  
40 functional *doublesex*. It is estimated that the role of the sex differentiation system for  
41 female phenotypes may have evolved through accumulating mutations in the protein  
42 motif structures that led to the enhancement of its transcription-regulatory function.  
43

## 44 **Introduction**

45           Sex is a fundamental principle in animal reproduction and is shared among  
46 almost all animals. The differences between males and females are a large source of  
47 diversity in mating systems, species, traits, and ecological dynamics in Metazoa  
48 (*Darwin, 1871; Fryzell et al., 2019; Geddes and Thomson, 1889*). The universality of  
49 sex suggests that sex is an ancient feature of metazoans. On the other hand, recent  
50 studies in various animals have revealed that regulatory systems for producing sex  
51 change rapidly during animal evolution (*Bachtrog et al., 2014; Beukeboom and*  
52 *Perrin, 2014; Herpin and Schartl, 2015*). For example, genes in the sex  
53 determination/sex differentiation systems are more likely to change upstream in the  
54 gene cascade than downstream (*Bopp et al., 2014; Wilkins, 1995*). In eutherian  
55 mammals such as mice and humans, a transcription factor called *Sex-determining*  
56 *region Y (Sry)* acts as a 'master regulator' of sex determination pathway, in which *Sry*  
57 induces expression of a transcriptional factor *doublesex and mab-3 related*  
58 *transcriptional factor 1 (dmrt1)* in males through chain reactions of transcription  
59 factors during embryogenesis (*Gubbay et al., 1990; Koopman et al., 1991; Miyawaki*  
60 *et al., 2020; Sinclair et al., 1991*). In contrast, in medaka fish, *Oryzias latipes*, a  
61 paralog of *dmrt1*, *dmy (DM-domain gene on the Y chromosome)* instead of *Sry*  
62 promotes male differentiation via a gene cascade inducing *dmrt1* (*Matsuda et al.,*  
63 *2002; Nanda et al., 2002*). The diversity in gene repertoires composing sex  
64 differentiation systems has also been found in arthropods (e.g., *Sharma et al., 2017;*  
65 *Suzuki et al., 2008; Xu et al., 2017*).

66           Diversity of sex differentiation systems has referred to differences in gene  
67 repertoires among species or populations. At present, many evolutionary scenarios

68 have been proposed to explain the evolutionary transition of gene repertoires in sex  
69 differentiation systems: e.g., neo-functionalization or sub-functionalization via gene  
70 duplication (e.g., *Chandler et al., 2017; Hattori et al., 2012; Hasselmann et al., 2008;*  
71 *Matsuda et al., 2002; Sharma et al., 2017; Yoshimoto et al., 2008*), positional  
72 exchange within the cascade via feedback loops (e.g., *Myosho et al. 2012; Myosho et*  
73 *al., 2015; Smith et al., 2009; Takehana et al., 2014*), and functional shifts via  
74 accumulation of mutations in *cis-* or *trans-*elements (e.g., *Kamiya et al., 2012; Sato et*  
75 *al., 2010*) (reviewed in *Beukeboom and Perrin, 2014*). Currently, most of the diversity  
76 of sex differentiation systems is explained by these well-understood scenarios for  
77 changes in gene repertoires. However, recently, a difference in sex differentiation  
78 systems without swapping gene repertoires has been discovered from pterygote  
79 insects.

80 Pterygote insects exhibit tremendous sexual dimorphisms in the head,  
81 abdomen, wings, and so on, realizing a complex mating strategy. Most of the sexual  
82 differences are produced by a sex differentiation system that uses a transcription  
83 factor *doublesex (dsx)*, a homolog of *dmrt1*) as a bottom factor (*Kopp, 2012; Verhulst*  
84 *and van de Zande, 2015*). Studies on Aparaglossata (holometabolan insects excluding  
85 Hymenoptera) have shown that *dsx* promotes both male and female differentiation via  
86 the sex-specific splicing (*Burtis and Baker 1989; Gotoh et al., 2016; Hildreth, 1964;*  
87 *Ito et al., 2013; Kijimoto et al., 2012; Ohbayashi et al., 2001; Shukla and Palli, 2012;*  
88 *Xu et al., 2017*). Recent studies showed that *dsx* promotes only male differentiation in  
89 several hemimetabolan and hymenopteran insects, even though *dsx* has sex-specific  
90 isoforms (*Mine et al., 2017; Takahashi et al., 2021; Wexler et al., 2015; Zhuo et al.,*  
91 *2018*). Thus, there is a difference in outputs in the sex differentiation systems in

92 insects: promoting only male differentiation (single-functionality) or both male and  
93 female differentiation (dual-functionality). It is suggested that the output of the insect  
94 sex differentiation systems transited from the single-functionality to the dual-  
95 functionality (Wexler *et al.*, 2019). However, it remains largely unclear how the  
96 difference in the output evolved independently of changes in gene repertoires and  
97 what drove such a transition (Hopkins and Kopp, 2021). Also, it is unidentified the  
98 ancestral roles of *dsx* isoforms in insects.

99         The evolutionary origin of the sex differentiation system in insects is  
100 ambiguous by the inability to estimate the status of the common ancestor of Insecta.  
101 All of the previous studies examining the *dsx* functionality have been limited to  
102 pterygote insects or crustaceans and chelicerates. In chelicerates and crustaceans, *dsx*  
103 has no sex-specific isoforms (Kato *et al.*, 2011; Li *et al.*, 2018; Panara *et al.*, 2019;  
104 Pomerantz *et al.*, 2015). We are currently forced to compare the status of crustaceans  
105 with that of pterygote insects, resulting in a large gap in phylogenetic mapping.  
106 Furthermore, previous reports of the single-functionality have been based mainly on  
107 the sexual differences acquired or complicated by each taxon in hemimetabolan  
108 insects. Therefore, it remains possible that the single-functionality reported so far  
109 results in a secondary loss of roles in female differentiation.

110         To address these issues, it is necessary to examine the function of *dsx* in taxa  
111 that retain the sexual traits of the common ancestor of Insecta and that emerged  
112 between the crustaceans and Pterygota. To this end, we focused on the firebrat  
113 *Thermobia domestica* (Zygentoma) belonging to Zygentoma, the sister group of  
114 Pterygota (Misof *et al.*, 2014). The sexual traits of *T. domestica* are restricted to the  
115 female simple ovipositor and the male ‘penis’ that is not aedeagus. These sexual traits

116 mirror the ancestral state of insects (*Beutel et al., 2017; Boudinot, 2018; Emeljanov,*  
117 *2014; Kristensen, 1975; Matsuda, 1976*). Here, to examine the exon-intron structure  
118 of *dsx*, we decoded the genome of *T. domestica*. Then, we developed the technology  
119 to effectively inhibit gene function during postembryonic development and  
120 investigated the roles of *dsx* for sexual traits, gametogenesis, and transcriptional  
121 regulation, and compared them with other insects.

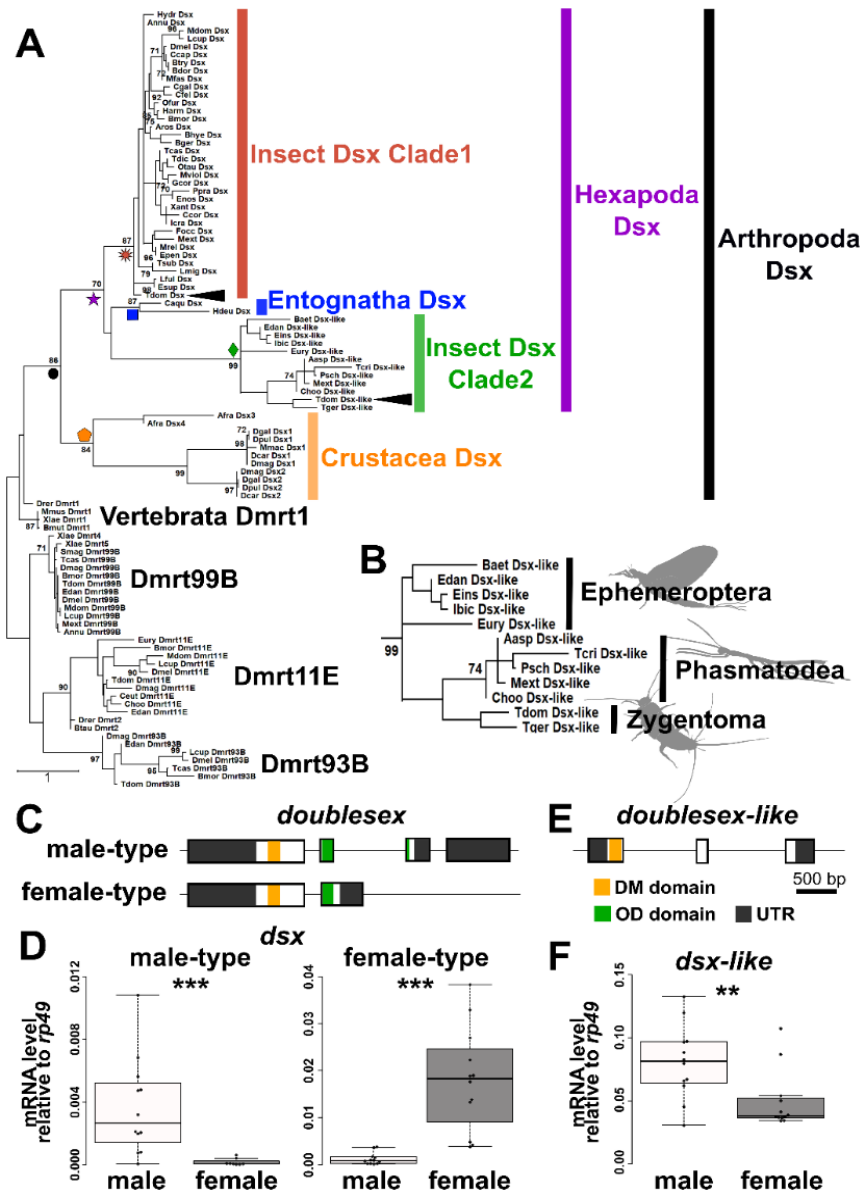
122

## 123 **Results**

### 124 **Molecular evolution of Doublesex in Pancrustacea**

125 First, we examined the relationship among *dsx* homologs in animals (Figure 1–  
126 figure supplement 1, Table 1) and revealed that the pancrustacean transcription factor  
127 *doublesex* (*dsx*) occurs in four clades: crustacean Dsx, Entognatha Dsx, Insect Dsx  
128 clade 1, and clade 2. (Figure 1A, B). *Thermobia domestica* has two *dsx* genes,  
129 belonging to different clades (Insect Dsx clade 1 and 2) (Figure 1–figure supplement  
130 2). We considered the gene belonging to Insect Dsx clade 1 to be an ortholog of the  
131 pterygote *dsx*, since this clade contains Dsx of pterygote insects including *Drosophila*  
132 *melanogaster*. We thus named the gene in Insect Dsx clade 2 *dsx-like* to distinguish it  
133 from *dsx*. Insect Dsx clade 2 contained *dsx-like* in Zygentoma as well as  
134 Ephemeroptera and Phasmatodea (Figure 1B), indicating that *dsx* was duplicated  
135 before the emergence of the Dicondylia (= Zygentoma + Pterygota) and was lost  
136 repeatedly in pterygote taxa. This fact supports that *T. domestica* retains the ancestral  
137 state for *dsx* related genes' contents. Since these results suggested the involvement of

138 the gene duplication in the functional evolution of *dsx*, we also analyzed the  
 139 expression and function of *dsx-like*.



140 **Figure 1.** Molecular evolution and features of Doublesex in *Thermobia domestica*. (A  
 141 to B) Molecular phylogeny of Doublesex and Mab-3 related transcriptional factors  
 142 (DMRT) (A) and enlarged view of insect Dsx Clade2 (*dsx-like* clade) (B). The  
 143 numerical value on each node is the bootstrap supporting value. Bootstrap values < 70  
 144 are not shown. The node of each clade is indicated by colored shapes: black circle,  
 145 Arthropoda Dsx; orange pentagon, Crustacea Dsx; purple star, Hexapoda Dsx; red  
 146 sunburst, Insect Dsx Clade1; green diamond, Insect Dsx Clade2; blue square,  
 147 Entognatha Dsx. (C to F) Molecular features of *dsx* (C and D) and *dsx-like* (E and F).  
 148 (C and E) indicate exon-intron structures of *dsx* and *dsx-like*, respectively. (D and F)  
 149 show mRNA expression levels of *dsx* and *dsx-like*, respectively. Each plot is a value  
 150 of an individual. Sample size is listed in Table 2. Results of Brunner–Munzel tests are  
 151 indicated by asterisks: \*\* $P < 0.01$ ; \*\*\* $P < 0.001$  and are described in Table 2.

152

153 **Sex-specific splicing regulation of *doublesex* in *Thermobia domestica***

154 We detected two major isoforms of *dsx* of *T. domestica* (Figure 1C). Mapping  
155 these sequences to our genome data showed that the longer (951 bp) and shorter (756  
156 bp) isoforms. Both isoforms shared a Doublesex and Mab-3 (DM) domain-containing  
157 exon, but differed in the 3'-terminus. The longer isoform was expressed at 40-fold  
158 higher levels in males than in females in the fat body. The shorter isoform was  
159 expressed in the fat body 18 times higher in females than in males (Figure 1D). We  
160 named thus the longer and shorter isoforms *dsx* male-type and *dsx* female-type,  
161 respectively. *dsx-like* was expressed two-fold more highly in males than in females  
162 (Figure 1F) but had no isoform (Figure 1E). Thus, *dsx* was regulated by a sex-specific  
163 splicing, whereas *dsx-like* was not under splicing control.

164 Before RNA interference (RNAi) analyses, we confirmed that expression  
165 levels of *dsx* and *dsx-like* mRNA were significantly reduced in *dsx* and *dsx-like* RNAi  
166 males and females. (Figure 1–figure supplement 3A and Table 2; see Materials and  
167 Methods section).

168 **Single-functionality of *doublesex* for phenotypic sex differentiation in *T.***  
169 ***domestica***

170 The sexual traits in *T. domestica* are the male penis and the female ovipositor  
171 (Figure 2A–D).

172 In *T. domestica* males, the penis is an unpaired appendix on the abdomen  
173 segment IX (*Matsuda, 1976*). The penis was sub-segmented into two parts. There  
174 were many setae on the left and the right side of the distal tips (Figure 2E, Figure2–  
175 figure supplement 1E). The surface of the penis had a reticulated pattern (Figure 2E,  
176 Figure2–figure supplement 1C, E). This simple penial structure was presumably  
177 gained at the last common ancestor of Ectognatha (*Boudinot, 2018*).

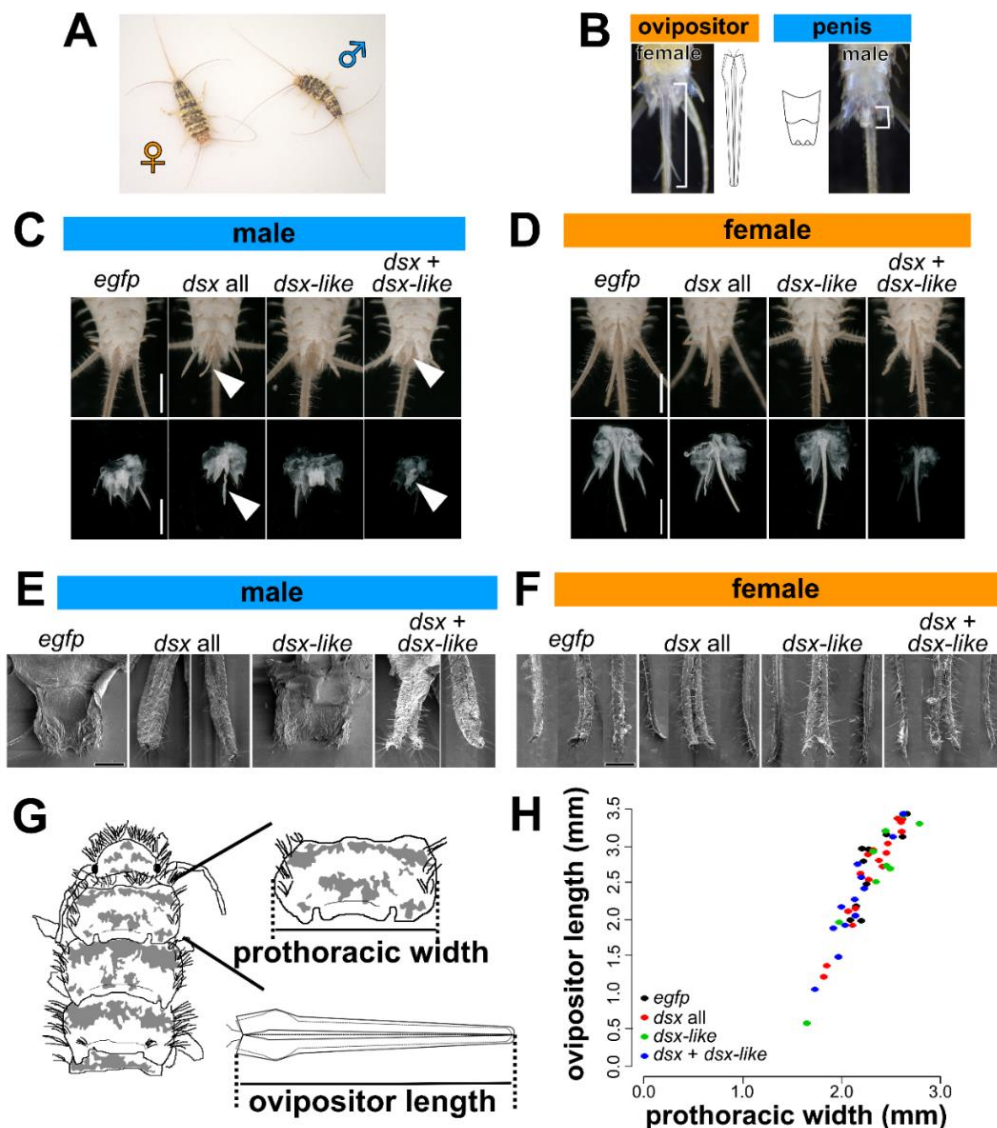


178 In *T. domestica* female, the ovipositor consists of two pairs of appendices  
179 (gonapophysis) and is derived from the retracted vesicles on the abdomen VIII and IX  
180 (Emeljanov, 2014; Matsuda, 1976). This ovipositor is an autapomorphy of Ectognatha  
181 (Beutel, 2017; Kristensen, 1975). The gonapophyses on the abdomen VIII (valvula I)  
182 were the ventral part of the ovipositor and a paired structure. The gonapophyses on  
183 the abdomen IX (valvula II) were the dorsal side of the ovipositor and were united to  
184 form an unpaired structure (Figure 2–figure supplement 2B). The distal tip of the  
185 valvula II remained a paired structure and possessed dense setae (Figure 2–figure  
186 supplement 2A). The valvula I was shorter than the valvula II (Figure 2–figure  
187 supplement 2A). Both valvulae were sub-segmented and have some setae (Figure 2F).  
188 The valvula I and II were connected through a tongue-and-groove structure  
189 (olistheter). The olistheter consisted of an aulax (“groove”) on the valvula I and a  
190 rhachis (“tongue”) on the valvula II (Figure 2–figure supplement 2B). Within the  
191 valvulae, the epithelial cells were beneath the cuticular layer. The cuticular layer was  
192 thickened and multi-layered in the outer surface of the ovipositor. In contrast, the  
193 inner surface (i.e., the side of the egg cavity) of the ovipositor had a thin and single-  
194 layered cuticle.

195 In *dsx* or *dsx* male-type RNAi males, a tubular organ was formed instead of  
196 the penis (Figure 2C, Figure2–figure supplement 1A). This tubular organ consisted of  
197 two pairs of appendage-like structures. The inner one is connected to the gonopore  
198 and the ejaculatory duct. The outer one had a lot of setae on its tip (Figure 2E,  
199 Figure2–figure supplement 1C, E). Thus, the inner pair was similar to the valvula I of  
200 the female ovipositor and the outer one was similar to the valvula II. These features  
201 indicated that the tubular organ in the *dsx* RNAi males was parallel to the female  
202 ovipositor. The same phenotype was found in the *dsx* and *dsx-like* double RNAi

203 males. In contrast, the *dsx-like* males possessed a penis the same as that of the control  
 204 insects.

205 In females that were treated with RNAi for *dsx*, *dsx* isoforms, *dsx-like*, or both  
 206 genes, the external genital organ was the same as the ovipositor of the control females  
 207 that described in the above section (Figure 2D, F, Figure 2–figure supplement 1B, D,  
 208 F, Figure2–figure supplement 2). Thus, in the view of histology, the location, and the  
 209 relation to other elements, the external organ of the RNAi females was not different  
 210 from the ovipositor of the control ones.



211 **Figure 2.** Function of Doublesex in sexually dimorphic traits in *Thermobia*  
 212 *domestica*. (A) A pair of *T. domestica*. The female looks much the same as the male.

213 (B) Sexually dimorphic traits of *T. domestica*. Females possess an ovipositor and  
214 males have a penis. (C to F) Phenotypes of *dsx* and *dsx-like* RNA interference (RNAi)  
215 individuals. Light microscopic image (C and D) and scanning electron microscopic  
216 image (E and F). Scales: 1 cm (C and D); 50  $\mu$ m (E and F). (G to H) Effect of *dsx* and  
217 *dsx-like* RNAi on the growth of the ovipositor. The ovipositor length was measured  
218 and is plotted with prothoracic width, an indicator of body size. The measurement  
219 scheme (G) and scatter plots (H). Each plot in (H) indicates a value of each individual.  
220 Sample size of (H) is listed in Table 4. Results of the generalized linear model  
221 analysis are listed in Table 4.

222

### 223 **No evidence for the effects of *doublesex* on female phenotypes in *T. domestica***

224 To investigate whether *dsx* in *T. domestica* females has functions other than  
225 female differentiation for phenotypes, we examined its role in the growth and  
226 maintenance of female organs (Figure 2G). We did not detect a significant difference  
227 in ovipositor length and prothoracic width, an indicator of body size, between the  
228 controls and the *dsx* and *dsx-like* RNA females (Figures 2H, Figure 2–figure  
229 supplement 3, Figure 2–figure supplement 4 and Table 4).

230 We then examined the effects of *dsx* on gonads, reproductive systems, and  
231 gametogenesis in *T. domestica*.

232 In males of *T. domestica*, a pair of testes was consisted of some testicular  
233 follicles (Figure 3A). Each testicular follicle was connected to the vas deferens via the  
234 vas efferens (Figure 3–figure supplement 1B). The seminal vesicle lay between the  
235 vas deferens and the ejaculatory duct. A pair of the ejaculatory ducts was associated  
236 with each other in the front of the gonopore in the penis (Figure 3C). The testicular  
237 follicles were a bean-like shape and the seminal vesicles were a bean pod-like shape.  
238 In the testicular follicle, the spermatogonia was in the antero-most part (Figures 3A).  
239 The primary and secondary spermatocytes lay in the middle part (Figures 3A). In the  
240 posterior part of the testicular follicle, there were some sperm bundles (Figures 3A).  
241 The wall of the testicular follicle consisted of a single flattened epithelial layer.

242 We observed the above features of the reproductive system in *dsx* or *dsx-like*  
243 RNAi males (Figure 3A and C). In *dsx* and both genes RNAi males, the seminal  
244 vesicles were round in shape. The vas efferens was filled with the sperm (Figure 3–  
245 figure supplement 1B). In contrast, we could not find differences in the morphology  
246 of the testicular follicles or spermatogenesis between the RNAi and control males.  
247 The male reproductive system and spermatogenesis showed no visible difference  
248 between *dsx* female-type and *dsx-like* RNAi females and the control ones.

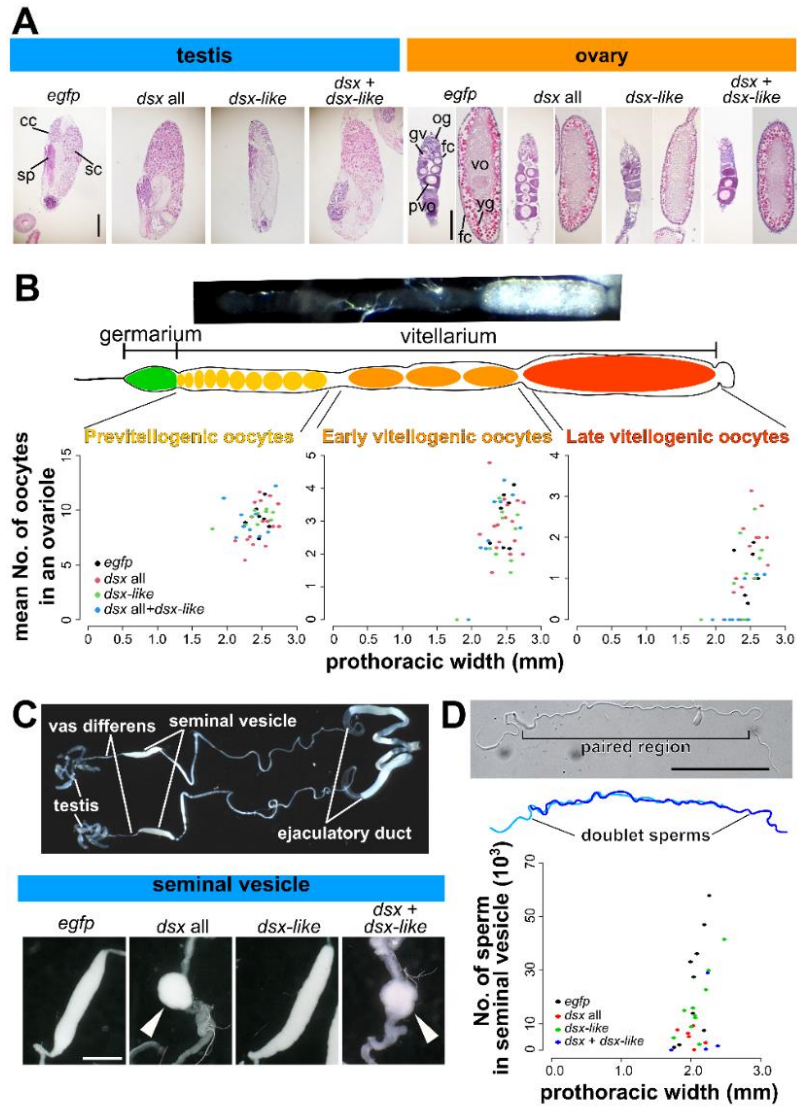
249 In females of *T. domestica*, each ovary consists of five ovarioles and was  
250 attached to the anterior part of the abdomen via the terminal tuft (Figure 3–figure  
251 supplement 1). The ovarioles were associated with each other at the lateral oviduct.  
252 The lateral oviduct was connected to the common oviduct and subsequently opened at  
253 the gonopore in the valvula I. There was no vagina between the gonopore and the  
254 oviduct. The spermatheca was located on the branch point of the common oviduct  
255 along the midline (Figure 3–figure supplement 1A). The spermatheca was divided  
256 into two parts: anterior and posterior (Figure 3–figure supplement 2). The anterior part  
257 consisted of a pseudostratified layer of the columnar epithelial cells that were  
258 secretory. The posterior part was surrounded by a single layer of epithelial cells. The  
259 ovariole was panoistic-type and was composed of two parts: the germarium and the  
260 vitellarium (Figure 3A, B). The germarium contained many oogonia and young  
261 oocytes. The vitellarium had previtellogenic and vitellogenic oocytes. The oocytes in  
262 the vitellarium were surrounded by a single layer of follicle cells. There were pedicel  
263 cells in the terminal of the ovariole. The previtellogenic oocyte had a large germinal  
264 vesicle and basophilic cytoplasm. The vitellogenic oocyte was elongated along the  
265 anterior-posterior axis of the ovariole and had eosinophilic cytoplasm. Many  
266 eosinophilic lipid droplets were present in the peripheral region of the vitellogenic

267 oocytes. The follicle cells were flattened and columnar in shape in the  
268 previtellogenesis and the vitellogenesis.

269 We observed the above features of the reproductive system in *dsx* or *dsx-like*  
270 RNAi females (Figures 3A, Figure 3–figure supplement 1, Figure 3–figure  
271 supplement 2). We could not detect differences in the female reproductive system or  
272 oogenesis between the RNAi females and the controls. This result suggests that the  
273 *dsx* and *dsx-like* have no function in the formation of female traits and gametogenesis  
274 at the tissue and cellular level.

275 Also, we were not able to detect any differences in the oocyte number and size  
276 between the controls and RNAi females (Figures 3B, Figure3–figure supplement 3  
277 and Table 4). However, the seminal vesicle in males became round in shape in the *dsx*  
278 RNAi males in contrast to the bean pod-like shape observed in the control males  
279 (Figures 3C, Figure3–figure supplement 1). We detected a significant reduction of the  
280 number of sperms within the seminal vesicle in *dsx* RNAi males (Figure 3D and Table  
281 5). *dsx* thus contributed to the development of the reproductive system and gametes in  
282 males, but not in females, of *T. domestica*.

283 Our results cannot show evidence for roles of *dsx* in *T. domestica* females.



284 **Figure 3.** Function of *doublesex* in reproductive systems and fecundity. (A) Effects of  
 285 *dsx* and *dsx-like* RNAi on gonad morphology and gametogenesis. In images of the  
 286 ovary, the left and right panel in each treatment show germarium/previtellogenesis  
 287 and vitellogenesis, respectively. cc, cystocyte; fc, follicle cell; gv, germinal vesicle;  
 288 og, oogonia; pvo, previtellogenic oocyte; sc, spermatocyte; sp, sperm; yg, yolk  
 289 granule; vo, vitellogenic oocyte. (B) The effect of *dsx* and *dsx-like* RNAi on oocyte  
 290 number in each oogenetic stage. The upper panels are images of an ovariole in *T.*  
 291 *domestica*. The lower panel shows scatter plots of oocyte numbers and prothoracic  
 292 width. Results of the generalized linear model analysis are in Tables 4 (female) and 5  
 293 (male). (C) The effect of *dsx* and *dsx-like* RNAi on the seminal vesicle. The upper  
 294 panel is a gross image of the male reproductive system. The lower one shows the  
 295 phenotype of each treatment. (D) The effect of *dsx* and *dsx-like* RNAi on sperm  
 296 number in seminal vesicles. The upper panels are images of sperm in *T. domestica*.  
 297 The sperm of *T. domestica* is usually paired with other sperm. The lower panel shows  
 298 a scatter plot of sperm numbers by prothoracic width. Scales: 50  $\mu$ m (A and C); 10  
 299  $\mu$ m (D). Sample size are also listed in Tables 4 (D) and 5 (C).

300

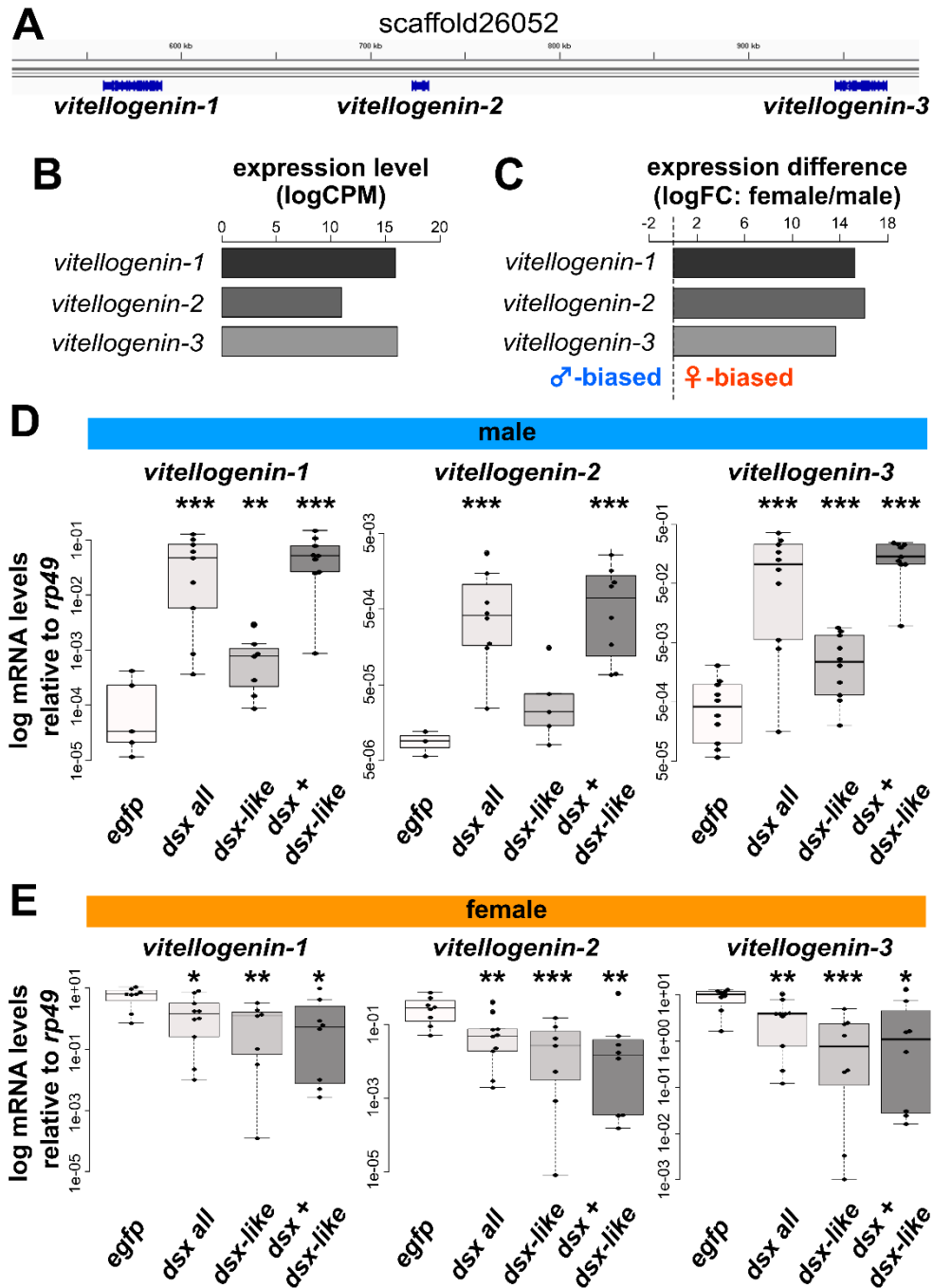
301 **Cryptic role of *doublesex* for female-specific transcripts in *T. domestica***

302 Previous studies in Hemimetabola (*Takahashi et al., 2021; Wexler et al., 2015;*  
303 *Zhuo et al., 2018*), and our results in *Zygentoma* show that *dsx* is not essential for the  
304 formation of female phenotypes in non-Holometabola. In contrast, considering the  
305 fact that the *dsx* female-specific isoform retains ORFs in non-Holometabola, there is a  
306 still possibility that *dsx* may have some function in non-holometabolan females. To  
307 investigate this functionality, we focused on the effect of *dsx* on female-specific gene  
308 expression.

309 We focused on the *vitellogenin (vtg)* gene, one of the major egg yolk proteins,  
310 which is specifically expressed in females of Bilateria (Byrne et al., 1989; *Hayward et*  
311 *al., 2010*). In the Holometabola, *dsx* promotes *vtg* mRNA expression in females and  
312 represses it in males (*Shukla and Palli, 2012; Suzuki et al., 2003; Thongsaiklaing et*  
313 *al., 2018*). Our RNA-seq analysis showed that levels of the three *vtg* mRNAs in *T.*  
314 *domestica* were more than 10000-fold higher in females than in males (Figure 4A–C).  
315 We found that the *vtg* mRNAs were expressed at 40–100-fold higher levels in *dsx*  
316 RNAi males than in the control males (Figure 4D and Table 2). Notably, the *dsx*  
317 RNAi females produced around half the amount of *vtg* mRNA as the controls. The  
318 *dsx-like* RNAi and a double-knockdown of *dsx* and *dsx-like* also significantly reduced  
319 the expression of *vtg* in females (Figure 4E and Table 2).

320 This result is the first case that *dsx* can promote female-specific *vitellogenin*  
321 expression in non-holometabolan species, even though it does not affect female  
322 phenotypes such as the oocyte size and number. This finding suggests that it has  
323 opposite functionality between males and females in *T. domestica* at the gene-  
324 regulatory level.

325



326 **Figure 4.** Function of *doublesex* in *vitellogenin* gene expression. (A to C) Features of  
 327 *vitellogenin* (*vtg*) genes of *Thermobia domestica*. An image of the *vtg* gene locus in an  
 328 Integrated Genome Viewer (A). The *vtg* genes are highly expressed in females (B and  
 329 C). The source data of B and C are provided as Figure4–source data 1. (D and E)  
 330 Effect of *dsx* and *dsx-like* RNAi on *vtg* genes' expression in males (D) and females  
 331 (E). The decreases were about 2/5–1/5, 1/10–3/50, and 1/9–1/20 in *dsx*, *dsx-like*, and  
 332 both the genes RNAi females. The mRNA expression levels are shown as logarithmic  
 333 scales. Each plot represents an individual. Sample sizes are listed in Table 2 (C and  
 334 D). Results of Brunner–Munzel tests are indicated by asterisks: \* $P < 0.05$ ; \*\* $P <$   
 335  $0.01$ ; \*\*\* $P < 0.001$  and is also described in Table 2.  $P > 0.05$  is not shown.  
 336



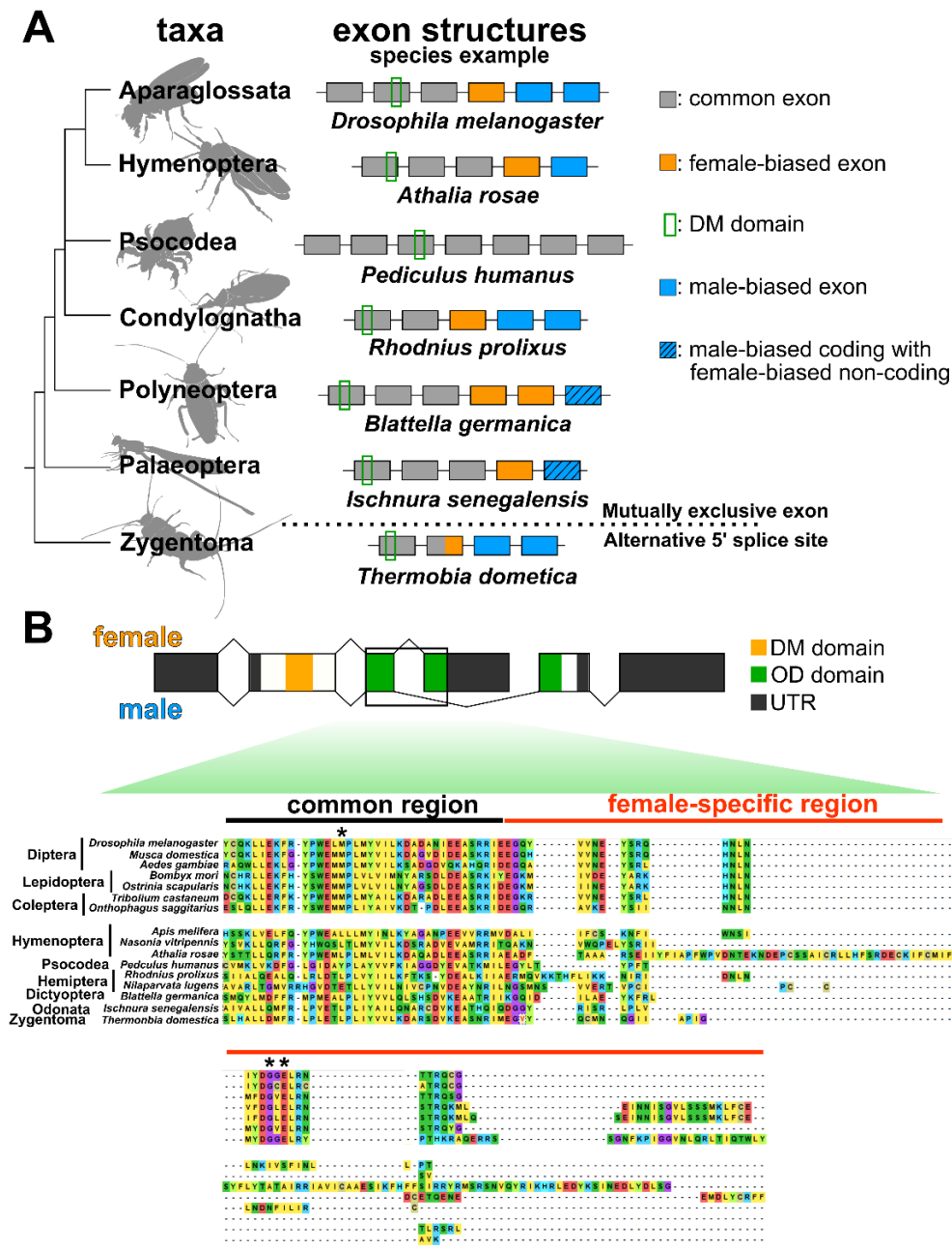
337 **Differences of *doublesex* sequences between single- and dual-functional species**

338 Genes can gain new functions due to gene duplication, co-factor function,  
339 changes in *cis*- or *trans*-region (Carroll, 2005; Ganformina and Sánchez, 1999; Mann  
340 and Carroll, 2002), or acquiring new exons. *dsx* paralog (*dsx-like*) found in this study  
341 did not contribute to female phenotypes (Figure 2 and 3). The female and male  
342 isoforms of *dsx* share the same DNA-binding domain, and *intersex*, a co-factor gene  
343 of *dsx*, contributes to the formation of female traits in *Nilaparvata lugens* (Zhang *et*  
344 *al.*, 2021), which has the single-functional *dsx*. These facts indicate that the gene  
345 duplication, neo-functionalization of co-factors, and changes in *cis*-regulatory  
346 elements are not likely to contribute to the evolution of the dual-functionality. Thus,  
347 we explored the remaining possibilities: novel exons or *trans*-regions.

348 We found that there are alternative splice types in *T. domestica*, which has an  
349 alternative 5' splice site, and in Pterygote insects, which have a mutually exclusive  
350 exon, but did not find any differences of exon structure between species with single-  
351 functionality of *dsx*, and those with dual-functionality (Figure 5A).

352 We finally discovered amino acid sequences in the female-specific region that  
353 differed between taxa with single- and dual-functionality of *dsx*. *dsx* isoforms are  
354 sexually different in the OD domain. This domain was divided into common, female-  
355 specific, and male-specific regions. Our multiple alignment analysis revealed that the  
356 female-specific region was highly conserved among the taxa with dual-functionality  
357 of *dsx*, but not among those with single functionality (Figures 5B, Figure 5–figure  
358 supplement 1). In contrast, the male-specific region was not highly conserved among  
359 the taxa with dual-functional *dsx* (Figure 5–figure supplement 2).

360



\*: conserved residues only in aparaglossatans

361 **Figure 5.** Comparisons of molecular features in *doublesex* among insect taxa. (A)  
 362 Exon structure of *dsx* among insect taxa. The coding region of *dsx* is shown. The  
 363 phylogenetic relationship is that of *Misof et al. (2014)* (B) amino acid sequence of  
 364 Dsx among insect taxa. The upper image shows the *dsx* structure of *Drosophila*  
 365 *melanogaster*. Asterisks indicate conserved residues in Aparaglossata.

366

## 367 **Discussion**

### 368 **A novel type of the output in the sex differentiation system**

369 We show that the *dsx* of *Thermobia domestica* is essential for producing male  
370 phenotypes, but does not contribute to female phenotypes. In contrast to the  
371 phenotypes, this study showed that the female-specific *vitellogenin* genes are slightly  
372 promoted by *dsx* in *T. domestica* females. These facts indicate that *dsx* in *T. domestica*  
373 has an opposite transcription-regulatory function in males and females. Therefore, in  
374 *T. domestica*, *dsx* contributes only to male differentiation at the phenotypic level, but  
375 affects both sexes at the transcription-regulatory level (seemingly useless nature).

376 There have been two known types of outputs of the insect sex differentiation  
377 system: one that can regulate feminization via both transcription-regulation and  
378 phenotypes, and one that cannot. The former is found in Diptera, Lepidoptera, and  
379 Coleoptera (e.g., Luo and Baker, 2015; Suzuki et al., 2003; Shukla and Palli, 2012),  
380 the latter in Dictyoptera and Hemimetabola (Wexler et al., 2019; Zhuo et al., 2018). In  
381 some species, such as the dung beetle *Onthophagus taurus*, *dsx* contributes only to  
382 male trait formation in some tissues (Ledón-Rettig et al., 2017). In these species, *dsx*  
383 is also responsible for producing traits of both sexes in other tissues. Therefore, it is  
384 likely that the former type is the primary capability of the sex differentiation systems  
385 in these species and that the function for promoting female differentiation may tissue-  
386 specifically become silent. In contrast, the seemingly useless nature of *dsx* for females  
387 in *T. domestica* is a third type of the insect sex differentiation system (Figure 6A).  
388 This third type indicates that phenotypic and transcription-regulatory levels do not  
389 necessarily coincide in the output of sex differentiation systems.

390 The sex differentiation systems of crustaceans, vertebrates, and nematodes  
391 have DMRT family transcription factors as bottom factors that are responsible for  
392 promoting male differentiation (*Kato et al., 2011; Kopp, 2012; Raymond et al., 1998;*  
393 *Raymond et al., 2000*). No hierarchical discrepancy has been found in the output of  
394 the sex differentiation system of these animals. Therefore, the output of the sex  
395 differentiation system in most animals can be classified into three categories: that are  
396 capable of contributing to 1) only masculinization (crustaceans, nematodes,  
397 vertebrates, Hemiptera, and Dictyoptera), 2) both masculinization and feminization  
398 (Diptera, Lepidoptera, and Coleoptera) or 3) both masculinization and feminization at  
399 the transcription-regulatory level but only masculinization at the phenotypic level (*T.*  
400 *domestica*).

#### 401 **On the origin of the sex-specific splicing of *doublesex***

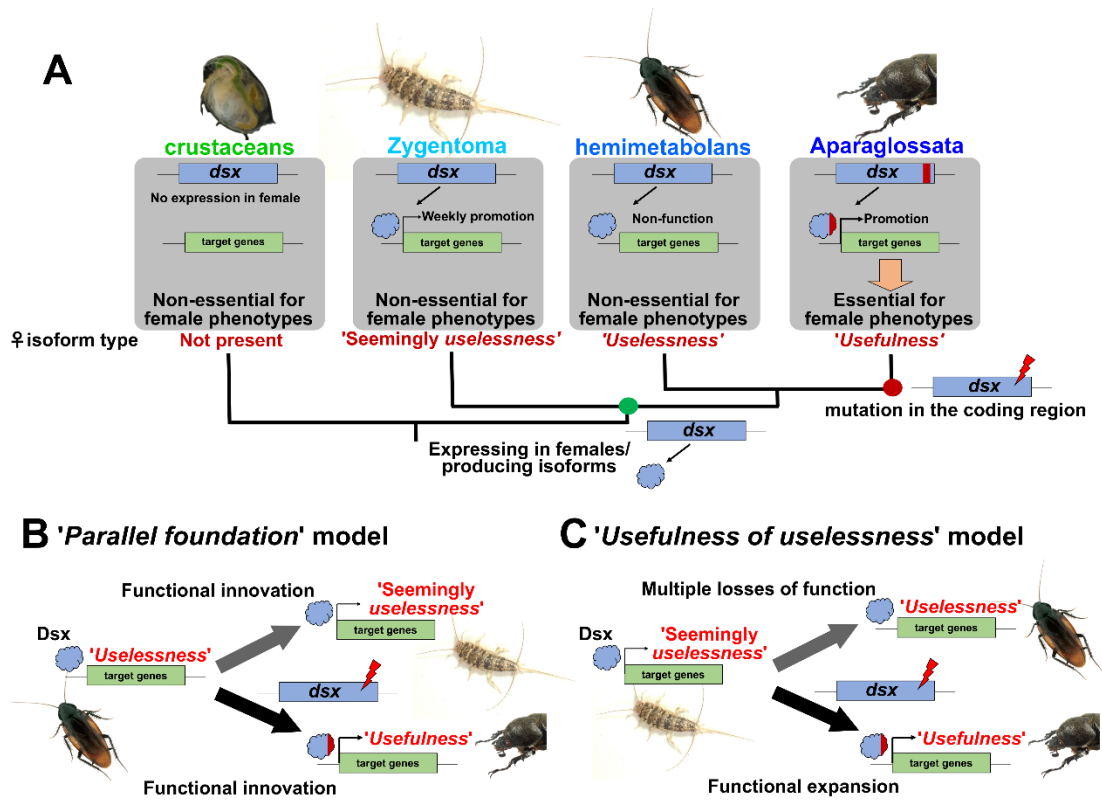
402 In pterygote insects (e.g., *Burtis and Baker, 1989; Shukla and Palli, 2012;*  
403 *Mine et al., 2017; Ohbayashi et al., 2001; Takahashi et al., 2019; Wexler et al., 2019;*  
404 *Zhuo et al., 2018*), *dsx* has sex-specific isoforms, except for a termite *Reticulitermes*  
405 *speratus* (*Miyazaki et al., 2021*). In contrast, *dsx* is controlled via a male-specific  
406 transcription in chelicerates and crustaceans (*Kato et al., 2011; Li et al., 2018; Panara*  
407 *et al., 2019; Pomerantz et al., 2015*). Here, sex-specific splicing regulation is  
408 observed in *dsx* of *T. domestica*, suggesting that sex-specific splicing regulation  
409 originated between the common ancestor of Branchiopoda and Hexapods and the  
410 common ancestor of Dicondylia (*Zygentoma* + Pterygota) (Figure 6A).

#### 411 **On the origin of the role of the insect sex differentiation system for females**

412 There are discrepancies in the output of the sex differentiation system in *T.*  
413 *domestica* at the phenotypic and transcription-regulatory levels. In such a case, it has

414 been proposed to map the characteristics of each hierarchical level separately on a  
 415 phylogenetic tree (c.f., *Abouheif, 1999*).

416



417

418 **Figure 6.** Evolutionary transition of outputs of the insect sex differentiation system.  
 419 (A) phylogenetic mapping of functionality of *dsx* for females. crustaceans: *Kato et al.*  
 420 (2011); Zygentoma: this study; hemimetabolans: *Wexler et al. (2019), Zhuo et al.*  
 421 (2018); Aparaglossata: e.g., *Shukla and Palli (2012), Suzuki et al. (2003)*. (B)  
 422 'Parallel foundation' model. (C) 'Usefulness of uselessness' model.

423

424 At the phenotypic level, previous studies have focused on taxon-specific or  
 425 highly complex sex differences, leaving open the possibility of a secondary loss of  
 426 function of *dsx* for females. However, the single-functionality of *dsx* even in *T.*  
 427 *domestica*, which has an ancestral, simple sex difference, supports a single origin for  
 428 *dsx* single-functionality. Based on a recent phylogenetic hypothesis (*Beutel et al.,*  
 429 *2017; Misof et al., 2014*), the transition from the single- to dual-functionality is  
 430 estimated to have occurred in the common ancestor of Aparaglossata (holometabolan

431 insects excluding Hymenoptera) (Figure 6A). At the phenotypic level, our findings  
432 ensure the evolutionary model by *Wexler et al. (2019)* that *dsx* initially acquired sex-  
433 specific isoforms and later became essential for female differentiation.

434 At the level of gene regulation, *dsx* in *T. domestica* can slightly promote the  
435 transcription of female-specific genes. Therefore, it is estimated that the common  
436 ancestor of Dicondylia already possessed the sexual dimorphic transcriptional control  
437 of *dsx*. In this case, it is inferred that the transcription-promoting function of female-  
438 specific genes was secondarily lost in hemimetabolan insects. Alternatively, it is  
439 possible that the common ancestor of the Dicondylia had also the single-functionality  
440 at the level of transcriptional regulation and that Zygentoma and Aparaglossata  
441 independently acquired the ability to promote transcription in females.

442 The question is how the function of *dsx* for the female phenotype evolved. We  
443 have found differences in the sequence of the female-specific region of *dsx* between  
444 phenotypically single-functional and dual-functional taxa. This region is located in the  
445 oligomerization (OD) domain, interacts with transcription factors (*An et al., 1995*;  
446 *Erdman et al., 1996*; *Ghosh et al., 2019*; *Romero-Pozuelo et al., 2019*) and  
447 transcriptional mediators such as *intersex* which is essential for female differentiation  
448 (*Gotoh et al., 2016*; *Morita et al., 2019*; *Xu et al., 2019*; *Yang et al., 2008*). Studies in  
449 *Blattella germanica* described low conservation of the OD domain (*Wexler et al.,*  
450 *2019*). *Baral et al. (2019)* also reported that the rate of non-synonymous substitutions  
451 in the female-specific region is low in Aparaglossata and high in Hymenoptera.  
452 However, the evolutionary significance of this region has been unclear. Our result  
453 suggests that the accumulation of mutations in female-specific regions has led to the  
454 female-differentiating functions at the phenotypic level (Figure 6). It was theoretically  
455 predicted that non-functional isoforms gain functions through mutation accumulation

456 in coding regions (*Keren et al., 2010*). The functional evolution of *dsx* in insects may  
457 fit this prediction.

### 458 **Evolutionary scenarios for the transition of the output of the sex differentiation** 459 **system**

460 In conclusion, we propose two alternative scenarios for the transition of the  
461 outputs of the insect sex differentiation system.

462 "*Parallel foundation*" hypothesis (Figure 6B): *dsx* has independently acquired the  
463 function for promoting female transcription in Zygentoma and Aparaglossata, and  
464 also gained the entirely novel role in phenotypic differentiation in females through the  
465 accumulation of coding mutations in Aparaglossata. This is the hypothesis that a  
466 useful functionality has arisen from a completely useless functionality.

467 "*Usefulness of uselessness*" hypothesis (Figure 6C): *dsx*, through the accumulation of  
468 mutations in its coding region, enhanced its weak transcription-promoting ability in  
469 females and became essential for producing the female phenotypes. This is the  
470 hypothesis that a useful functionality arose from a seemingly useless functionality.

471 Both these hypotheses can explain the diversity in outputs of the sex  
472 differentiation system via the accumulation of coding mutations in existing genes.  
473 Thus, a heterotypic evolution may drive the evolution of outputs of the sex  
474 differentiation systems. Textbook examples of the heterotypic evolution include a  
475 mutation of human *hemoglobin  $\beta$*  leading to sickle cells and coding mutations of  
476 *Ultrabithorax* that resulted in suppressed leg development in insects (reviewed in  
477 *Arthur, 2010; Gilbert, 2013; Futuyma and Kirkpatrick, 2017*). So far, heterotypy at  
478 the molecular level is considered as the change in the molecular function leading to  
479 entirely novel or no functions from existing functions of the molecule in phenotypes.  
480 On the other hand, the female isoform of *dsx* shows no function in female phenotypes.

481 Our hypotheses are models that a non-functional isoform gains functionality at the  
482 phenotypic level. The heterotypic evolution may need to be divided into modification  
483 from existing functions and innovation from non-functionality at phenotypic level.

484 In this study, we succeeded in detecting the transcription-promoting ability of  
485 *dsx* in females by examining the expression of *vitellogenin*. In hemimetabolan insects.  
486 the transcription-promoting function in females has not been found in *vitellogenin*  
487 (*Wexler et al., 2019; Zhuo et al., 2018*), but might be detected in other female-specific  
488 genes. Future comprehensive examination of the effects of *dsx* by transcriptome and  
489 comparisons at the mega-evolutionary level, i.e., higher taxa than families (*Arthur,*  
490 *2003*), using broad insect taxa will test these hypotheses.

491

## 492 **Materials and Methods**

### 493 **Animals**

494 A firebrat, *Thermobia domestica* (Packard, 1873), was used as an emerging model  
495 apterygote. *T. domestica* is one of the species belonging to the Zygentoma  
496 (Lepismatidae). The insects were kept at 37°C in total darkness condition and fed with  
497 fish food (TetraFin Goldfish Flakes, Tetra GmbH, Melle, Germany) in our laboratory.  
498 Stock colonies were reared in plastic cases of 30 cm×40 cm or 18 cm × 25 cm in  
499 length. Eggs were collected from tissue paper in the case and incubated at 37°C. For  
500 nymphal RNAi analysis, colonies of hatched nymphs were reared up to the fourth  
501 instar in a six-well plate and then transferred into 24-well plates to be kept  
502 individually. For adult RNAi analysis, adult insects were collected from the stock  
503 colony and transferred into the plates. For nymphal RNAi analysis, we used firebrats  
504 from April to June, 2019, February to April, April to July, and September to



505 December, 2020. For adult RNAi, adult firebrats were manipulated from June to July,  
506 2020.

### 507 **Estimation of molt timing**

508 Estimating the molt timing of insects is essential for the analysis of  
509 developmental processes and the functions of developmental regulatory genes. The  
510 timing of Hemi- or holometabolan insects can be estimated using morphological  
511 changes such as a wing growth. However, timing is hard to estimate in apterygote  
512 insects since they have little change in their morphology during postembryonic  
513 development. *T. domestica* forms scales in the fourth instar, and changes the number  
514 and length of its styli during the fourth to ninth instar under our breeding conditions.  
515 These features can be used to estimate molt timing, but it is difficult to apply these  
516 criteria to experiments using adults or a large number of nymphs. To resolve this  
517 problem, we used leg regeneration after autotomy and time-lapse imaging to estimate  
518 the molt timing of *T. domestica*. Autotomy occurs at the joint between the trochanter  
519 and femur in *T. domestica*. An autotomized leg regenerates after one molt (*Buck and*  
520 *Edwards, 1990*). For nymphal RNAi analysis, we amputated a right hindleg at the  
521 autotomic rift, using tweezers, and observed whether the leg had regenerated. This test  
522 enabled us to rapidly estimate the molt timing. For adult RNAi, time-lapse imaging  
523 was used to determine the precise time of molt. We build a time-lapse imaging system  
524 with a network camera system (SANYO, Tokyo, Japan) set in an incubator at 37°C  
525 (Figure 4–figure supplement 1A). Photos of insects in the 24-well plate were taken  
526 every five minutes. We created a time-lapse movie from the photos every 12 hours  
527 using ImageJ 1.52a (<https://imagej.nih.gov/ij/>) and observed whether the insects  
528 molted (Figure 4–figure supplement 1B, Video 1).

### 529 **De novo genome assembly**

530 A whole genome of *T. domestica* was sequenced to analyze the exon-intron  
531 structure of *dsx*. We selected an adult female of *T. domestica* from our stock colony  
532 and removed its alimentary canal. Genomic DNA was extracted from the sample  
533 using DNeasy Blood and Tissue Kit (QIAGEN K.K., Tokyo, Japan). A paired-end  
534 library was constructed from 1 µg of the DNA using TruSeq DNA PCR-Free LT  
535 Sample Prep kits (Illumina K.K., Tokyo, Japan) following the manufacturer's  
536 instructions. The library was run on a sequencer (HiSeq 2500; Illumina K.K., Tokyo,  
537 Japan). We obtained 417 Gb of raw reads and assembled them using Platanus v1.2.4  
538 assembler (Kajitani *et al.*, 2014) after removal of the adapter sequences.

### 539 **Transcriptome analysis**

540 To search for *doublesex* (*dsx*) and *vitellogenin* (*vgt*) homologs, we performed  
541 RNA-seq analysis. Adults of 15 ♀♀ and 15 ♂♂ of *T. domestica* were sampled 1440  
542 minutes after a molt in December, 2019. The fat bodies of the individuals were  
543 removed using tweezers in a phosphated buffered saline (PBS; pH=7.2). Three adults  
544 were used per sample. Total RNA was extracted from 10 samples (5 ♀♀, 5 ♂♂) using  
545 RNeasy Micro kits (QIAGEN K.K., Tokyo, Japan) following the manufacturer's  
546 instructions. The concentration of purified RNA was measured using a Qubit 4  
547 fluorometer (QIAGEN K.K., Tokyo, Japan) with Qubit RNA BR Assay kits  
548 (QIAGEN K.K., Tokyo, Japan). Paired-end libraries were constructed from 100 ng of  
549 the total RNAs using TruSeq RNA Library Prep kits v2 (Illumina K.K., Tokyo,  
550 Japan) following the manufacturer's instructions. The libraries were run on a  
551 sequencer (HiSeq, Illumina, Tokyo, Japan). The library preparation and sequencing  
552 were performed by Genewiz Strand-Specific RNA-seq service. We mapped the reads  
553 obtained to the assembled genome using the HISAT2 program (Kim *et al.*, 2019) with  
554 a default option and counted the mapped reads using the STRINGTie program

555 (Pertea, 2015) with default parameter settings. Differential expression gene analysis  
556 was performed based on the count matrix using the “edgeR” package (Robinson *et al.*,  
557 2010) in R-v4.0.3 (R Core Team, 2020). Information about the samples can be  
558 obtained from the National Center for Biotechnology Information (NCBI) BioSample  
559 database (Accession number: SAMN18175012–SAMN18175021).

#### 560 **Molecular phylogenetic analysis**

561 Dsx is a member of the Doublesex and Mab-3 Related transcriptional factors  
562 (DMRT) family, and has a DNA binding domain, Doublesex and Mab-3 (DM)  
563 domain. Pancrustacea generally has four DMRT family genes, Dsx, Dmrt11,  
564 Dmrt93B, and Dmrt99B (Mawaribuchi *et al.*, 2019). Phylogenetic analysis of Dsx  
565 homologs was performed using the amino acid sequences of the DM domain. We  
566 used the Dsx sequences of *D. melanogaster* as a query and obtained 97 metazoan  
567 DMRT family proteins from the NCBI and the i5k databases  
568 (<https://i5k.nal.usda.gov/>) and our genome data of *T. domestica* by the BLAST  
569 analysis (listed in Table 1). We then aligned the sequences using MAFFT version 7  
570 (Kato *et al.*, 2013) with the -linsi option (to use an accuracy option, L-INS-i) and  
571 manually extracted the DM domain, which consisted of 61 amino acids (Figure 1–  
572 figure supplement 1). Molecular phylogenetic analysis of the aligned sequences was  
573 performed using a maximum likelihood method after selecting a substitution model  
574 (JTT matrix-based model) with MEGA X (Kumar *et al.*, 2018). Bootstrap values were  
575 calculated after 1000 replications.

#### 576 **Full-length cDNA and exon-intron structures**

577 To elucidate the exon-intron structures of Dsx and Dsx-like, we determined  
578 the full-length cDNA sequences using a Rapid Amplification of cDNA Ends (RACE)  
579 method and performed a BLAST analysis for our genome database of *T. domestica*.

580 We extracted total RNA from eggs, whole bodies, fat body, and gonads of nymphs  
581 and adult females and males of *T. domestica* using TRI Reagent (Molecular Research  
582 Center Inc., Ohio, USA) following the manufacturer's instructions. The total RNAs  
583 were treated with RNase-Free DNase I (New England BioLabs Japan Inc., Tokyo,  
584 Japan) to exclude remaining genomic DNA and purified by phenol/chloroform  
585 extraction and ethanol precipitation. For 5' -RACE analysis, mRNAs were purified  
586 from 75 µg of the total RNAs using Dynabeads mRNA Purification kit (Thermo  
587 Fisher Scientific K.K., Tokyo, Japan) following the manufacturer's instruction. We  
588 then ligated an RNA oligo at the 5'-end of the mRNA using GeneRacer Advanced  
589 RACE kits (Thermo Fisher Scientific K.K., Tokyo, Japan). For 3'-RACE analysis, we  
590 ligated an RNA oligo of the SMART RACE cDNA Amplification Kit (Takara Bio  
591 Inc., Shiga, Japan) at 3'-end of the total RNA during reverse transcription. First  
592 stranded (fs-) cDNA was generated from the RNAs using SuperScript III Reverse  
593 Transcriptase (Thermo Fisher Scientific K.K., Tokyo, Japan). We used primers  
594 specific to the RNA oligos and performed RACE analysis by nested RT-PCR using  
595 Q5 High-Fidelity DNA polymerase (New England BioLabs Japan Inc., Tokyo,  
596 Japan). The primers specific to *dsx* and *dsx-like* were made from sequences of the  
597 relevant genomic regions and are listed in Table 6. The amplicons were separated  
598 using the agarose gel-electrophoresis and cloned using TOPO TA Cloning Kit for  
599 Sequencing (Thermo Fisher Scientific K.K., Tokyo, Japan) following the  
600 manufacture's protocol. We used a DH5α *Escherichia coli* strain (TOYOBO CO.,  
601 LTD., Osaka, Japan) as the host cell. Plasmids were extracted using the alkaline lysis  
602 and purified by phenol-chloroform and ethanol precipitation. The nucleotide  
603 sequences of the cloned amplicons were determined from the purified plasmids by the  
604 Sanger Sequencing service of FASMAC Co. Ltd. (Kanagawa, Japan). We then

605 searched the genomic region of the full-length cDNA sequences of *dsx* and *dsx-like*  
606 via local blastn analysis.

### 607 **Reverse transcription-quantitative PCR (RT-qPCR)**

608 To quantitative mRNA expression levels, we performed RT-qPCR analysis.  
609 For investigating the sex-specific expression profile of *dsx* and *dsx-like*, we used the  
610 fat body of adults of *T. domestica* since the sexes can be distinguishable by the  
611 external morphology at this stage. Fat bodies also exhibit sex-specific physiological  
612 functions in adults. Thirteenth instar individuals and adults after molting were  
613 sampled for nymphal and adult RNAi analyses, respectively. The sample sizes are  
614 reported in the Table 2. We dissected the individuals in PBS and collected their fat  
615 body in 2 ml tubes containing TRI Reagent (Molecular Research Center Inc., Ohio,  
616 USA). The fat bodies then were disrupted using a TissueLyser LT small beads mill  
617 (QIAGEN K.K., Tokyo, Japan). These disrupted samples were preserved at  $-80^{\circ}\text{C}$   
618 until used. Total RNA was extracted from the samples according to the manufacture's  
619 protocol for the TRI Reagent. Extracted RNA was treated with 2% RNase-free DNase  
620 I (New England BioLabs Japan Inc., Tokyo, Japan) at  $37^{\circ}\text{C}$  for 40 minutes and  
621 purified by phenol/chloroform extraction and ethanol precipitation. We measured the  
622 concentration of the total RNA using a spectrophotometer (DS-11+, Denovix Inc.,  
623 Wilmington, USA). fs-cDNA was synthesized from 350 ng of the total RNA using  
624 SuperScript III Reverse Transcriptase (Thermo Fisher Scientific K.K., Tokyo, Japan).  
625 We diluted the fs-cDNA to 1:2 with MilliQ water and preserved it at  $-30^{\circ}\text{C}$  until it  
626 was used in RT-qPCR assay. The RT-qPCR assays were performed using a  
627 LightCycler 96 instrument (Roche, Basel, Switzerland) according to the  
628 manufacture's protocol with the THUNDERBIRD SYBR qPCR Mix (TOYOBO Co.  
629 Ltd., Osaka, Japan). The reaction volume was 10  $\mu\text{l}$ . We used 1  $\mu\text{l}$  of the fs-cDNA as

630 templates. The preparation of the RT-qPCR solution proceeded on ice. The protocol  
631 of the RT-qPCR was as follows: preincubation at 95°C for 600 seconds and 45 cycles  
632 of three-step reactions, such as denaturation at 95°C for 15 seconds, annealing at 60°C  
633 for 15 seconds and extension at 72°C for 45 seconds. We used *ribosomal protein 49*  
634 (*rp49*) as a reference gene, as described by *Ohde et al. (2011)*. We designed primer  
635 sets of the target genes by the Primer3Web version 4.1.0 (*Untergasser et al., 2012*)  
636 following the manufacture’s recommended condition of the THUNDERBIRD SYBR  
637 qPCR Mix. We confirmed the primers’ specificity using melting curves ranging from  
638 65°C to 95°C. We selected primer sets exhibiting a single peak. The primers are listed  
639 in Table 6. Each RT-qPCR was technically replicated three times. Some samples were  
640 excluded before analyzing the data when the Ct value of any genes was not detected  
641 (ND) in one or more replicates or when the Ct value of the reference gene deviated  
642 from that of other samples. In these removed data, a technical error was suspected.  
643 We calculated the expression level of target genes by the  $2^{-\Delta\Delta Ct}$  method (*Livak and*  
644 *Schmittgen, 2001*) and performed the Brunner–Munzel (BM) test for  $\Delta Ct$  value. The  
645 BM test was carried out using R-v4.0.3. with the *brunnermuzel.test* function of the  
646 “brunnermuzel” package ([https://cran.r-](https://cran.r-project.org/web/packages/brunnermunzel/index.html)  
647 [project.org/web/packages/brunnermunzel/index.html](https://cran.r-project.org/web/packages/brunnermunzel/index.html)). Holm’s method was used for  
648 multiple comparison analyses between the control and treatments. The data are listed  
649 in Table 2. Also, its source data can be found in Table2–Source Data 1. In the *dsx*  
650 expression of the RNAi male, we performed the Smirnov-Grubbs (SG) test for  $\Delta Ct$   
651 value using the *grubbs.test* function of the “outliers” package in R ([https://cran.r-](https://cran.r-project.org/web/packages/outliers/index.html)  
652 [project.org/web/packages/outliers/index.html](https://cran.r-project.org/web/packages/outliers/index.html)) (Table 3). An outlier was detected in  
653 the *dsx* RNAi male. We repeatedly performed the SG test using the data excluding the

654 outlier. No further outliers were detected. Lastly, we re-analyzed the data, excluding  
655 the outlier, using the BM test (Table 2).

## 656 **RNAi analysis**

657 Nymphal RNAi can be used to analyze the roles of genes during  
658 postembryonic development. The sexual differentiation of insects is generally  
659 assumed to be a cell-autonomous mechanism that is independent of systemic  
660 hormonal- control (*Verhulst and van de Zande, 2015*) as discussed in *De Loof and*  
661 *Huybrechts (1998)* and *Bear and Monteiro (2013)* and progresses during  
662 postembryonic development. Therefore, nymphal RNAi is the most effective tool to  
663 investigate the roles of genes on sexual trait formation. To reduce the possibility of  
664 off-target effects, the dsRNA was designed to avoid the region of the DM domain. We  
665 also confirmed that the dsRNA had no contiguous matches of more than 20 bases with  
666 other regions of the genome. To produce templates for the dsRNA, we cloned the  
667 regions of *dsx* and *dsx-like* from the fs-cDNA using the same method as the RACE  
668 analysis. We amplified the template DNAs from purified plasmids with PCR using  
669 Q5 High-Fidelity DNA Polymerase and purified the amplified DNA with the  
670 phenol/chloroform extraction and the ethanol precipitation. dsRNA was synthesized  
671 from the purified DNA using Ampliscribe T7-Flash Transcription kits (Epicentre  
672 Technologies, Co., Wisconsin, USA). We designed the PCR primers using the  
673 Primer3Web version 4.1.0 (*Untergasser et al., 2012*). The PCR primers are listed in  
674 Table 6. In nymphal RNAi analysis, we injected the dsRNAs repeatedly into the  
675 abdomen of the nymphs of *T. domestica* with each molt from the fourth or fifth instar  
676 to thirteenth instar to sustain the RNAi effect during postembryonic development. The  
677 initial stage was the same within a single experiment. This repeated nymphal RNAi  
678 was effective in some insects such as *Blattella germanica* (*Wexler et al., 2014*). We

679 sampled the individuals one, three, and five days after molting, using phenotypic  
680 observations, analysis of *dsx* knockdown effects, and the oocyte size and number. To  
681 determine the sex of individuals, we initially observed the gonads: testis and ovary. In  
682 our nymphal RNAi analysis, the gonads completely formed and there was no  
683 difference between the control and *dsx* RNAi individuals in external morphology  
684 (Figures 1–figure supplement 3, Figure2–figure supplement 1A). Therefore, at least in  
685 this assay, the gonad morphology was effective for the identification of the sex of *dsx*  
686 RNAi individuals. Individuals with testis were males and those with ovaries were  
687 females. For the analysis of *vtg* genes, we used the adult RNAi assay. *T. domestica*  
688 molts throughout its life, even after sexual maturation, and produces *vtg* during each  
689 adult instar (*Rouset and Bitsch, 1993*). In the adult RNAi analysis, we injected dsRNA  
690 repeatedly into the adults every three days. The dsRNA was initially injected into  
691 adults 12 hours after molting. We sampled the adults at  $720\pm 20$  minutes after  
692 subsequently molts, to analyze the *vtg* mRNA levels.

### 693 **Phenotype observation**

694 We dissected thirteenth instar individuals in PBS using tweezers and removed  
695 the thoraxes, reproductive systems, and external genital organs. We took images using  
696 the digital microscope system (VHX-5000, KEYENCE, Tokyo, Japan). The thoraxes  
697 and external genital organs were fixed with FAA fixative (formaldehyde: ethanol:  
698 acetic acid = 15:5:1) at 25°C overnight and then preserved in 90% ethanol. We used  
699 the length of the prothorax as an indicator of body size. To measure the prothoracic  
700 width, the prothoracic notum was removed from the fixed thorax after treatment with  
701 10% NaOH solution at 60°C for 30 minutes to dissolve the soft tissues. The notum  
702 was mounted in Lemosol on a microscope slide. The prepared specimens were imaged  
703 using a KEYENCE VHX-5000. With the microscope at 50×, the length of the notum



704 was measured. The ovipositor length and oocyte size were also measured using the  
705 microscope at 20× and 50×. The oocyte size was taken to be the major length of the  
706 late vitellogenic oocyte at the posterior most part of the ovariole. To count the sperm  
707 number, sperm was collected from seminal vesicles and diluted with 5 ml MilliQ  
708 water. 50 µl of the diluted sperm was spotted on a microscope slide and dried  
709 overnight. We technically replicated the measurement three times for ovipositor  
710 length and six times in sperm number and calculated these means. Measurement was  
711 performed by blinding the treatment. We counted the number of oocytes in ovarioles  
712 using an optical microscope at 50× (Olympus, Tokyo, Japan). A generalized linear  
713 model (GLM) was used to analyze differences in ovipositor length and oocyte size  
714 (length data) and sperm and oocyte number (count data) among RNAi treatments. The  
715 body size, target genes, and interactions between the target genes were used as  
716 explanatory variables. The length was assumed to follow a Gaussian distribution, and  
717 the count data to have a negative binomial distribution. We used R-v4.0.3 in these  
718 analyses and the *glm* and the *glm.nb* (MASS package) functions for the length and  
719 count data, respectively. To analyze the contribution of the explanatory variables, a  
720 likelihood ratio test for the result of GLM was performed using the *Anova* function of  
721 the *car* package. The statistical results are listed in Tables 4 (female) and 5 (male).  
722 Also, the source data are reported in Table 4—source data 1 and Table 5—source data 1.

### 723 **Scanning Electron Microscopy (SEM)**

724 The NanoSuit method (*Takaku et al., 2013*) was used for the SEM analysis. Male  
725 penises and female ovipositors preserved in 90% ethanol were washed with distilled  
726 water and immersed in 1% Tween20 at 25°C for 10 minutes. The samples were  
727 mounted on stubs and imaged using a low-vacuum SEM (DX-500; KEYENCE,  
728 Tokyo, Japan).

729 **Histology**

730 The gonads of RNAi individuals were fixed with Bouin's fixative (saturated picric  
731 acid: formaldehyde: glacial acetic acid = 15:5:1) at 25°C overnight and washed with  
732 90% ethanol plus Lithium Carbonate (Li<sub>2</sub>CO<sub>3</sub>). The ovipositors of RNAi individuals  
733 were fixed with FAA fixative at 25°C overnight and then were transferred into 90%  
734 ethanol. The samples were dehydrated and cleared with an ethanol-butanol series. The  
735 cleared samples were immersed and embedded in paraffin at 60°C. The paraffin  
736 blocks were polymerized at 4°C and cut into 5 µm thick sections using a microtome  
737 (RM2155: Leica, Wetzlar, Germany). The sections were mounted on microscope  
738 slides coated with egg white-glycerin and stained using Delafield's Hematoxylin and  
739 Eosin staining. The stained slides were enclosed with Canada balsam. We observed  
740 the slides on an optical microscope (Olympus, Tokyo, Japan) and took photos using a  
741 digital single-lens reflex camera (Nikon, Tokyo, Japan).

742 **Comparison of exon-intron structure and amino acid sequences**

743 We obtained exon-intron structures of *dsx* in seven insect species from NCBI. The  
744 female- and male-specific regions were visualized as red and blue colors, respectively.  
745 The exon-intron structures were mapped on a phylogenetic hypothesis based on *Misof*  
746 *et al. (2014)*. We obtained amino acid sequences of Dsx isoforms of 10 species from  
747 the NCBI database. *Wexler et al. (2014)* showed that *dsx* of *Pediculus humanus*  
748 (Psocodea) has isoforms without sex-specificity. In this study, based on the blast  
749 search and exon structure, we determined that PhDsx1 in *Wexler et al. (2019)*  
750 corresponded to the *dsx* female-type and PhDsx2 to *dsx* male-type. The sequences  
751 were aligned using MAFFT version 7 with a -linsi option.

752 **Data availability**

753 The draft genome data was deposited in the DNA Data Bank of Japan (Accession  
754 number: DRA005797; Bioproject: PRJDB5781). The raw read data of the  
755 transcriptome was in the NCBI Sequence Read Archive (Accession numbers:  
756 SRR13870115–SRR13870124; Bioproject: PRJNA707122). The sequences of *dsx*  
757 male-type, *dsx* female-type, and *dsx-like* are also in GenBank (Accession numbers:  
758 MW711323, MW711324, and MW711325, respectively).

759

## 760 **Acknowledgments**

761 We would like to thank Dr. Takahiro Ohde (National Institute for Basic Biology;  
762 Kyoto University) for his help to extract genomic DNA of *T. domestica* and for a  
763 great advice to the discussion. We are also grateful to Dr. Toshiya Ando, Dr. Taro  
764 Nakamura, Dr. Shinichi Morita, Dr. Hiroki Sakai, and Dr. Tatsuro Konagaya  
765 (National Institute for Basic Biology) for technical advice and discussion on this  
766 manuscript. We also express our gratitude to Dr. Morita for providing a photo of  
767 *Daphnia magna*. Computations were performed on the NIG supercomputer at ROIS,  
768 National Institute of Genetics and the Data Integration and Analysis Facility, National  
769 Institute for Basic Biology. We thank the Model Plant Research Facility, NIBB  
770 Bioresource Center for providing the network camera system. This work was  
771 supported by the JSPS KAKENHI Grant numbers JP25660265, JP16H02596, and  
772 JP16H06279 (PAGS) for TN and the Sasakawa Scientific Research Grant from The  
773 Japan Science Society for YC.

774

## 775 **Author Contributions:**

776 YC and TN conceived this study. YC performed the cloning of *dsx* and *dsx-like*, the  
777 RNAi, the RNA-seq, and the molecular phylogenetic analysis. AT sequenced the  
778 genome. MO and TI performed the de novo genome assembly. YC and T. wrote this  
779 manuscript; all authors commented on the manuscript.

780

## 781 **Competing Interest Statement**

782 The authors declare that have no competing interests.

783

## 784 **References**

- 785 Abouheif E. 1999. A method for testing the assumption of phylogenetic independence  
786 in comparative data. *Evolutionary Ecology Research* **1**: 895–909.
- 787 An W, Wensink PC. 1995. Integrating sex-and tissue-specific regulation within a  
788 single *Drosophila* enhancer. *Genes & Development* **9**: 256–266.
- 789 Arthur W. 2003. Micro-, Macro-, and Megaevolution In: Hall BK, Olson WM (Eds).  
790 *Keywords and Concepts in Evolutionary Developmental Biology*. Cambridge:  
791 Harvard University Press. p. 249–260.
- 792 Arthur W. 2010. *Evolution: A Developmental Approach*. New York: John Wiley &  
793 Sons.
- 794 Bachtrog D, Mank JE, Peichel CL, Kirkpatrick M, Otto SP, Ashman TL, Hahn MW,  
795 Kitano J, Mayrose I, Ming R, Perrin N, Ross L, Valenzuela N, Vamosi JC, Tree of  
796 Sex Consortium. 2014. Sex determination: why so many ways of doing it? *PLoS*  
797 *Biol* **12**: e1001899.

- 798 Baral S, Arumugam G, Deshmukh R, Kunte K. 2019. Genetic architecture and sex–  
799 specific selection govern modular, male–biased evolution of *doublesex*. *Science*  
800 *Advances* **5**: eaau3753.
- 801 Bear A, Monteiro A. 2013. Both cell-autonomous mechanisms and hormones  
802 contribute to sexual development in vertebrates and insects. *Bioessays* **35**: 725–  
803 732.
- 804 Beukeboom LW, Perrin N. 2014. *The evolution of sex determination*. Oxford: Oxford  
805 University Press.
- 806 Beutel RG, Yavorskaya MI, Mashimo Y, Fukui M, Meusemann K. 2017. The  
807 phylogeny of Hexapoda (Arthropoda) and the evolution of megadiversity.  
808 *Proceedings of the Arthropodan Embryological Society of Japan* **51**: 1–15.
- 809 Bopp D, Saccone G, Beye M. 2014. Sex determination in insects: variations on a  
810 common theme. *Sexual Develoepment* **8**: 20–28.
- 811 Boudinot BE. 2018. A general theory of genital homologies for the Hexapoda  
812 (Pancrustacea) derived from skeletomuscular correspondences, with emphasis on  
813 the Endopterygota. *Arthropod Structure & Development* **47**: 563–613.
- 814 Buck C, Edwards JS. 1990. The effect of appendage and scale loss on instar duration  
815 in adult firebrats, *Thermobia domestica* (Thysanura). *Journal of Experimental*  
816 *Biology* **151**: 341–347.
- 817 Burtis KC, Baker BS. 1989. *Drosophila doublesex* gene controls somatic sexual  
818 differentiation by producing alternatively spliced mRNAs encoding related sex–  
819 specific polypeptides. *Cell* **56**: 997–1010.
- 820 Byrne BM, Gruber MABG, Ab G. 1989. The evolution of egg yolk proteins. *Progress*  
821 *in Biophysics & Molecular Biology* **53**: 33–69.

- 822 Carroll SB. 2005. Evolution at Two Levels: On Genes and Form. *PLoS Biol.* **3**:e245.
- 823 Chandler JC, Fitzgibbon QP, Smith G, Elizur A, Ventura T. 2017. *Y-linked iDmrt1*  
824 paralogue (*iDMY*) in the Eastern spiny lobster, *Sagmariasus verreauxi*: The first  
825 invertebrate sex-linked *Dmrt*. *Developmental Biology* **430**: 337–345.
- 826 Darwin C. 1871. *The Descent of Man, and Selection in Relation to Sex vol. 1* London:  
827 John Murray.
- 828 De Loof A, Huybrechts R. 1998. “Insects do not have sex hormones”: a myth?  
829 *General and Comparative Endocrinology* 111: 245–260.
- 830 Emeljanov AF. 2014. The evolutionary role and fate of the primary ovipositor in  
831 insects. *Entomological Review* **94**: 367–396.
- 832 Erdman SE, Chen HJ, Burtis KC. 1996. Functional and genetic characterization of the  
833 oligomerization and DNA binding properties of the *Drosophila doublesex* proteins.  
834 *Genetics* **144**: 1639–1652.
- 835 Fryxell DC, Weiler DE, Kinnison MT, Palkovacs EP. 2019. Eco–evolutionary  
836 dynamics of sexual dimorphism. *Trends in Ecology and Evolution* **34**: 591–594.
- 837 Futuyma D, Kirkpatrick M. 2017. *Evolution 4th edition* Sunderland: Sinauer  
838 Associates.
- 839 Ganfornina MD, Sánchez D. 1999. Generation of evolutionary novelty by functional  
840 shift. *Bioessays* **21**: 432–439.
- 841 Geddes P, Thomson JA. 1889. *The evolution of sex*. London: Walter Scott.
- 842 Gempe T, Hasselmann M, Schjøtt M, Hause G, Otte M, Beye M. 2009. Sex  
843 determination in honeybees: two separate mechanisms induce and maintain the  
844 female pathway. *PLoS Biol.* **7**: e1000222.

- 845 Ghosh N, Bakshi A, Khandelwal R, Rajan SG, Joshi R. 2019. The Hox gene  
846 *Abdominal-B* uses Doublesex<sup>F</sup> as a cofactor to promote neuroblast apoptosis in the  
847 *Drosophila* central nervous system. *Development* **146**: dev175158.
- 848 Gilbert SF. 2013. *Developmental Biology 10th edition*. Sunderland: Sinauer  
849 Associates.
- 850 Gotoh H, Zinna RA, Warren I, DeNieu M, Niimi T, Dworkin I, Emlen DJ, Miura T,  
851 Lavine LC. 2016. Identification and functional analyses of sex determination genes  
852 in the sexually dimorphic stag beetle *Cyclommatus metallifer*. *BMC Genomics* **17**:  
853 250.
- 854 Gubbay J, Collignon J, Koopman P, Capel B, Economou A, Münsterberg A, Vivian  
855 N, Goodfellow P, Lovell-Badge R. 1990. A gene mapping to the sex-determining  
856 region of the mouse Y chromosome is a member of a novel family of  
857 embryonically expressed genes. *Nature* **346**: 245–250.
- 858 Hasselmann M, Gempe T, Schiøtt M, Nunes-Silva CG, Otte M, Beye M. 2008.  
859 Evidence for the evolutionary nascence of a novel sex determination pathway in  
860 honeybees. *Nature* **454**: 519–522.
- 861 Hattori, Y. Murai, M. Oura, S. Masuda, S. K. Majhi, T. Sakamoto, J. I. Hattori RS,  
862 Murai Y, Oura M, Masuda S, Majhi SK, Sakamoto T, Fernandino JI, Somoza GM,  
863 Yokota M, Strüssmann CA. 2012. A Y-linked anti-Müllerian hormone duplication  
864 takes over a critical role in sex determination. *PNAS* **109**: 2955–2959.
- 865 Hayward A, Takahashi T, Bendena WG, Tobe SS, Hui JH. 2010. Comparative  
866 genomic and phylogenetic analysis of vitellogenin and other large lipid transfer  
867 proteins in metazoans. *FEBS Letters* **584**: 1273–1278.

- 868 Herpin A, Schartl M. 2015. Plasticity of gene-regulatory networks controlling sex  
869 determination: of masters, slaves, usual suspects, newcomers, and usurpators.  
870 *EMBO Reports* **16**: 1260–1274.
- 871 Hildreth PE. 1965. Doublesex, a recessive gene that transforms both males and  
872 females of *Drosophila* into intersexes. *Genetics* **51**: 659–678.
- 873 Hopkins BR, Kopp A. 2021. Evolution of sexual development and sexual dimorphism  
874 in insects. *Current Opinion in Genetics & Development* **69**: 129–139.
- 875 Ito Y, Harigai A, Nakata M, Hosoya T, Araya K, Oba Y, Ito A, Ohde T, Yaginuma T,  
876 Niimi T. 2013. The role of *doublesex* in the evolution of exaggerated horns in the  
877 Japanese rhinoceros beetle. *EMBO Reports* **14**: 561–567.
- 878 Luo SD, Baker BS. 2015. Constraints on the evolution of a *doublesex* target gene  
879 arising from *doublesex*'s pleiotropic deployment. *PNAS* **112**: 852–861.
- 880 Kamiya T, Kai W, Tasumi S, Oka A, Matsunaga T, Mizuno N, Fujita M, Suetake H,  
881 Suzuki S, Hosoya S, Tohari S, Brenner S, Miyadai T, Venkatesh B, Suzuki Y,  
882 Kikuchi K. 2012. A trans-species missense SNP in *Amhr2* is associated with sex  
883 determination in the tiger pufferfish, *Takifugu rubripes* (fugu). *PLoS Genetics* **8**:  
884 e1002798.
- 885 Kajitani R, Toshimoto K, Noguchi H, Toyoda A, Ogura Y, Okuno M, Yabana M,  
886 Harada M, Nagayasu E, Maruyama H, Kohara Y, Fujiyama A, Hayashi T, Itoh T.  
887 2014. Efficient de novo assembly of highly heterozygous genomes from whole-  
888 genome shotgun short reads. *Genome Reserach* **24**:1384–95.
- 889 Kato Y, Kobayashi K, Watanabe H, Iguchi T. 2011. Environmental sex determination  
890 in the branchiopod crustacean *Daphnia magna*: deep conservation of a *Doublesex*  
891 gene in the sex-determining pathway. *PLOS Genet.* **7**: e1001345.



- 892 Katoh K, Standley DM. 2013. MAFFT multiple sequence alignment software version  
893 7: improvements in performance and usability. *Molecular Biology and Evolution*  
894 **30**: 772–780.
- 895 Keren H, Lev-Maor G, Ast G. 2010. Alternative splicing and evolution:  
896 diversification, exon definition and function. *Nature Review Genetics* **11**: 345–355.
- 897 Kijimoto T, Moczek AP, Andrews J. 2012. Diversification of *doublesex* function  
898 underlies morph-, sex-, and species-specific development of beetle horns. *PNAS*  
899 **109**: 20526–20531.
- 900 Kim D, Paggi JM, Park C, Bennett C, Salzberg SL. 2019. Graph-based genome  
901 alignment and genotyping with HISAT2 and HISAT-genotype. *Nature*  
902 *Biotechnology* **37**: 907–915.
- 903 Koopman P, Gubbay J, Vivian N, Goodfellow P, Lovell-Badge R. 1991. Male  
904 development of chromosomally female mice transgenic for *Sry*. *Nature* **351**: 117–  
905 121.
- 906 Kopp A. 2012. *Dmrt* genes in the development and evolution of sexual dimorphism.  
907 *Trends in Genetics* **28**: 175–184.
- 908 Kristensen NP. 1975. The phylogeny of hexapod “orders”. A critical review of recent  
909 accounts. *Journal of Zoological Systematics and Evolutionary Research* **13**: 1–44.
- 910 Kumar S, Stecher G, Li M, Knyaz C, Tamura K. 2018. MEGA X: molecular  
911 evolutionary genetics analysis across computing platforms. *Molecular Biology and*  
912 *Evolution* **35**: 1547–1549.
- 913 Ledón-Rettig C, Zattara E, Moczek A. 2017. Asymmetric interactions between  
914 *doublesex* and tissue- and sex-specific target genes mediate sexual dimorphism in  
915 beetles. *Nature Communications* **8**: 14593.

- 916 Li S, Li F, Yu K, Xiang J. 2018. Identification and characterization of a *doublesex*  
917 gene which regulates the expression of insulin-like androgenic gland hormone in  
918 *Fenneropenaeus chinensis*. *Gene* **649**: 1–7.
- 919 Livak KJ, Schmittgen TD. 2001. Analysis of relative gene expression data using real–  
920 time quantitative PCR and the  $2^{-\Delta\Delta CT}$  method. *Methods* **25**: 402–408.
- 921 Mann RM, Carroll SB. 2002. Molecular mechanisms of selector gene function and  
922 evolution. *Current Opinion in Genetics & Development* **5**: 592–600.
- 923 Matsuda M, Nagahama Y, Shinomiya A, Sato T, Matsuda C, Kobayashi T, Morrey  
924 CE, Shibata N, Asakawa S, Shimizu N, Hori H, Hamaguchi S, Sakaizumi M. 2002.  
925 DMY is a Y-specific DM-domain gene required for male development in the  
926 medaka fish. *Nature* **417**: 559–563.
- 927 Matsuda R. 1976. *Morphology and Evolution of the Insect Abdomen: With Special*  
928 *Reference to Developmental Patterns and their Bearings upon Systematics*.  
929 Oxford: Pergamon Press.
- 930 Mawaribuchi S, Ito Y, Ito M. 2019. Independent evolution for sex determination and  
931 differentiation in the DMRT family in animals. *Biology Open* **8**: bio041962.
- 932 McQueen E, Rebeiz M. 2020. On the specificity of gene regulatory networks: How  
933 does network co-option affect subsequent evolution? *Current Topics in*  
934 *Developmental Biology* **139**: 375–405.
- 935 Mine S, Sumitani M, Aoki F, Hatakeyama M, Suzuki MG. 2017. Identification and  
936 functional characterization of the sex-determining gene *doublesex* in the sawfly,  
937 *Athalia rosae* (Hymenoptera: Tenthredinidae). *Applied Entomology and Zoology*  
938 **52**: 497–509.
- 939 Misof B, Liu S, Meusemann K, Peters RS, Donath A, Mayer C, Frandsen PB, Ware J,  
940 Flouri T, Beutel RG, Niehuis O, Petersen M, Izquierdo-Carrasco F, Wappler T,

941 Rust J, Aberer AJ, Aspöck U, Aspöck H, Bartel D, Blanke A, Berger S, Böhm A,  
942 Buckley TR, Calcott B, Chen J, Friedrich F, Fukui M, Fujita M, Greve C, Grobe P,  
943 Gu S, Huang Y, Jermin LS, Kawahara AY, Krogmann L, Kubiak M, Lanfear R,  
944 Letsch H, Li Y, Li Z, Li J, Lu H, Machida R, Mashimo Y, Kapli P, McKenna DD,  
945 Meng G, Nakagaki Y, Navarrete-Heredia JL, Ott M, Ou Y, Pass G, Podsiadlowski  
946 L, Pohl H, von Reumont BM, Schütte K, Sekiya K, Shimizu S, Slipinski A,  
947 Stamatakis A, Song W, Su X, Szucsich NU, Tan M, Tan X, Tang M, Tang J,  
948 Timelthaler G, Tomizuka S, Trautwein M, Tong X, Uchifune T, Walz MG,  
949 Wiegmann BM, Wilbrandt J, Wipfler B, Wong TK, Wu Q, Wu G, Xie Y, Yang S,  
950 Yang Q, Yeates DK, Yoshizawa K, Zhang Q, Zhang R, Zhang W, Zhang Y, Zhao  
951 J, Zhou C, Zhou L, Ziesmann T, Zou S, Li Y, Xu X, Zhang Y, Yang H, Wang J,  
952 Wang J, Kjer KM, Zhou X. 2014. Phylogenomics resolves the timing and pattern  
953 of insect evolution. *Science* **346**: 763–767.

954 Miyawaki S, Kuroki S, Maeda R, Okashita N, Koopman P, Tachibana M. 2020. The  
955 mouse *Sry* locus harbors a cryptic exon that is essential for male sex determination.  
956 *Science* **370**, 121–124.

957 Miyazaki S, Fujiwara K, Kai K, Masuoka Y, Gotoh H, Niimi T, Hayashi Y,  
958 Shigenobu S, Maekawa K. 2021. Evolutionary transition of *doublesex* regulation in  
959 termites and cockroaches: from sex-specific splicing to male-specific transcription.  
960 *bioRxiv*.

961 Morita S, Ando T, Maeno A, Mizutani T, Mase M, Shigenobu S, Niimi T. 2019.  
962 Precise staging of beetle horn formation in *Trypoxylus dichotomus* reveals the  
963 pleiotropic roles of *doublesex* depending on the spatiotemporal developmental  
964 contexts. *PLOS Genetics* **15**: e1008063.

- 965 Myosho T, Takehana Y, Hamaguchi S, Sakaizumi M. 2015. Turnover of sex  
966 chromosomes in celebensis group medaka fishes. *G3: Genes, Genomes, Genetics*  
967 **5**: 2685–2691.
- 968 Myosho T, Otake H, Masuyama H, Matsuda M, Kuroki Y, Fujiyama A, Naruse K,  
969 Hamaguchi S, Sakaizumi M. 2012. Tracing the emergence of a novel sex-  
970 determining gene in medaka, *Oryzias luzonensis*. *Genetics* **191**: 163–170.
- 971 Nanda I, Kondo M, Hornung U, Asakawa S, Winkler C, Shimizu A, Shan Z, Haaf T,  
972 Shimizu N, Shima A, Schmid M, Schartl M. 2002. A duplicated copy of DMRT1  
973 in the sex-determining region of the Y chromosome of the medaka, *Oryzias latipes*.  
974 *PNAS* **99**: 11778–11783.
- 975 Ohbayashi F, Suzuki MG, Mita K, Okano K, Shimada T. 2001. A homologue of the  
976 *Drosophila doublesex* gene is transcribed into sex-specific mRNA isoforms in the  
977 silkworm, *Bombyx mori*. *Comparative Biochemistry and Physiology - Part B:*  
978 *Biochemistry & Molecular Biology* **128**: 145–158.
- 979 Ohde T, Yaginuma T, Niimi T. 2011. Nymphal RNAi analysis reveals novel function  
980 of scalloped in antenna, cercus and caudal filament formation in the firebrat,  
981 *Thermobia domestica*. *Journal of Insect Biotechnology and Sericology* **80**: 101–  
982 108.
- 983 Panara V, Budd GE, Janssen R. 2019. Phylogenetic analysis and embryonic  
984 expression of panarthropod Dmrt genes. *Frontiers in Zoology* **16**: 1–18.
- 985 Perteua M, Perteua GM, Antonescu CM, Chang TC, Mendell JT, Salzberg SL. 2015.  
986 StringTie enables improved reconstruction of a transcriptome from RNA-seq reads.  
987 *Nature Biotechnology* **33**: 290–295.
- 988 Pomerantz AF, Hoy MA, Kawahara AY. 2015. Molecular characterization and  
989 evolutionary insights into potential sex-determination genes in the western orchard

- 990 predatory mite *Metaseiulus occidentalis* (Chelicerata: Arachnida: Acari:  
991 Phytoseiidae). *Journal of Biomolecular Structure and Dynamics* **33**: 1239–1253.
- 992 Raymond CS, Murphy MW, O'Sullivan MG, Bardwell VJ, Zarkower D. 2000. *Dmrt1*,  
993 a gene related to worm and fly sexual regulators, is required for mammalian testis  
994 differentiation. *Genes & Development* **14**: 2587–2595.
- 995 Raymond CS, Shamu CE, Shen MM, Seifert KJ, Hirsch B, Hodgkin J, Zarkower D.  
996 1998. Evidence for evolutionary conservation of sex-determining genes. *Nature*,  
997 **391**, 691–695.
- 998 R Core Team. 2020. *R: A language and environment for statistical computing*. R  
999 Foundation for Statistical Computing.
- 1000 Robinson MD, McCarthy DJ, Smyth GK. 2010. edgeR: a Bioconductor package for  
1001 differential expression analysis of digital gene expression data. *Bioinformatics* **26**:  
1002 139–140.
- 1003 Romero-Pozuelo J, Foronda D, Martín P, Hudry B, Merabet S, Graba Y, Sánchez-  
1004 Herrero E. 2019. Cooperation of axial and sex specific information controls  
1005 *Drosophila* female genitalia growth by regulating the Decapentaplegic pathway.  
1006 *Developmental Biology* **454**: 145–155.
- 1007 Rousset A., Bitsch C. 1993. Comparison between endogenous and exogenous yolk  
1008 proteins along an ovarian cycle in the firebat *Thermobia domestica* (Insecta,  
1009 Thysanura). *Comparative Biochemistry and Physiology Part B: Biochemistry and*  
1010 *Molecular Biology* **104**: 33–44.
- 1011 Sato Y, Shinka T, Sakamoto K, Ewis AA, Nakahori Y. 2010. The male-determining  
1012 gene *SRY* is a hybrid of *DGCR8* and *SOX3*, and is regulated by the transcription  
1013 factor *CP2*. *Molecular and Cellular Biochemistry* **337**: 267–275.

- 1014 Sharma A, Heinze SD, Wu Y, Kohlbrenner T, Morilla I, Brunner C, Wimmer EA, van  
1015 de Zande L, Robinson MD, Beukeboom LW, Bopp D. 2017. Male sex in  
1016 houseflies is determined by *Mdmd*, a paralog of the generic splice factor gene  
1017 *CWC22*. *Science* **356**: 642–645.
- 1018 Shukla JN, Palli SR. 2012. Doublesex target genes in the red flour beetle, *Tribolium*  
1019 *castaneum*. *Scientific Reports* **2**: 948.
- 1020 Sinclair AH, Berta P, Palmer MS, Hawkins JR, Griffiths BL, Smith MJ, Foster JW,  
1021 Frischauf AM, Lovell-Badge R, Goodfellow PN. 1990. A gene from the human  
1022 sex-determining region encodes a protein with homology to a conserved DNA-  
1023 binding motif. *Nature* **346**: 240–244.
- 1024 Smith CA, Roeszler KN, Ohnesorg T, Cummins DM, Farlie PG, Doran TJ, Sinclair  
1025 AH. 2009. The avian Z-linked gene *DMRT1* is required for male sex determination  
1026 in the chicken. *Nature* **461**: 267–271.
- 1027 Suzuki MG, Funaguma S, Kanda T, Tamura T, Shimada T. 2003. Analysis of the  
1028 biological functions of a *doublesex* homologue in *Bombyx mori*. *Developmental*  
1029 *Genes and Evolution* **213**: 345–354.
- 1030 Suzuki MG, Imanishi S, Dohmae N, Nishimura T, Shimada T, Matsumoto S. 2008.  
1031 Establishment of a novel in vivo sex-specific splicing assay system to identify a  
1032 trans-acting factor that negatively regulates splicing of *Bombyx mori dsx* female  
1033 exons. *Molecular and Cellular Biology* **28**: 333–343.
- 1034 Takaku Y, Suzuki H, Ohta I, Ishii D, Muranaka Y, Shimomura M, Hariyama T. 2013.  
1035 A thin polymer membrane, nano-suit, enhancing survival across the continuum  
1036 between air and high vacuum. *PNAS* **110**:7631–7635.

- 1037 Takahashi M, Okude G, Futahashi R, Takahashi Y, Kawata M. 2021. The effect of  
1038 the *doublesex* gene in body colour masculinization of the damselfly *Ischnura*  
1039 *senegalensis*. *Biology Letters* **17**: 20200761.
- 1040 Takahashi M, Takahashi Y, Kawata M. 2019. Candidate genes associated with color  
1041 morphs of female-limited polymorphisms of the damselfly *Ischnura senegalensis*.  
1042 *Heredity* **122**: 81–92.
- 1043 Takehana Y, Matsuda M, Myosho T, Suster ML, Kawakami K, Shin-I T, Kohara Y,  
1044 Kuroki Y, Toyoda A, Fujiyama A, Hamaguchi S, Sakaizumi M, Naruse K. 2014.  
1045 Co-option of *Sox3* as the male-determining factor on the Y chromosome in the fish  
1046 *Oryzias dancena*. *Nature Communications* **5**: 4157.
- 1047 Thongsaklaing T, Passara H, Nipitwathanaphon M, Ngernsiri L. 2018. Identification  
1048 and characterization of *doublesex* from the pumpkin fruit fly, *Bactrocera tau*  
1049 (Diptera: Tephritidae). *European Journal of Entomology* **115**: 602–613.
- 1050 True JR, Carroll SB. 2002. Gene co-option in physiological and morphological  
1051 evolution. *Annual Review of Cell and Developmental Biology* **18**: 53–80.
- 1052 Untergasser A, Cutcutache I, Koressaar T, Ye J, Faircloth BC, Remm M, Rozen SG.  
1053 2012. Primer3--new capabilities and interfaces. *Nucleic Acids Research* **40**: e115.
- 1054 Verhulst EC, van de Zande L. 2015. Double nexus—Doublesex is the connecting  
1055 element in sex determination. *Briefings in Functional Genomics* **14**: 396–406.
- 1056 Verhulst EC, van de Zande L, Beukeboom LW. 2010. Insect sex determination: it all  
1057 evolves around *transformer*. *Current Opinion in Genetics & Development* **20**:  
1058 376–383.
- 1059 Wexler J, Delaney EK, Belles X, Schal C, Wada-Katsumata A, Amicucci MJ, Kopp  
1060 A. 2019. Hemimetabolous insects elucidate the origin of sexual development via  
1061 alternative splicing. *eLife* **8**: e47490.

- 1062 Wexler JR, Plachetzki DC, Kopp A. 2014. Pan-metazoan phylogeny of the DMRT  
1063 gene family: a framework for functional studies. *Developmental Genes and*  
1064 *Evolution* **224**: 175–181.
- 1065 Wilkins AS. 1995. Moving up the hierarchy: a hypothesis on the evolution of a  
1066 genetic sex determination pathway. *Bioessays* **17**: 71–77.
- 1067 Xu J, Chen S, Zeng B, James AA, Tan A, Huang Y. 2017. *Bombyx mori* P-element  
1068 *Somatic Inhibitor (BmPSI)* is a key auxiliary factor for silkworm male sex  
1069 determination. *PLoS Genetics* **13**: e1006576.
- 1070 Xu J, Yu Y, Chen K, Huang Y. 2019. *Intersex* regulates female external genital and  
1071 imaginal disc development in the silkworm. *Insect Biochemistry and Molecular*  
1072 *Biology* **108**: 1–8.
- 1073 Xu J, Zhan S, Chen S, Zeng B, Li Z, James AA, Tan A, Huang Y. Sexually dimorphic  
1074 traits in the silkworm, *Bombyx mori*, are regulated by *doublesex*. 2017. *Insect*  
1075 *Biochemistry and Molecular Biology* **80**: 42–51.
- 1076 Yang Y, Zhang W, Bayrer JR, Weiss MA. 2008. Doublesex and the regulation of  
1077 sexual dimorphism in *Drosophila melanogaster*: structure, function, and  
1078 mutagenesis of a female-specific domain. *Journal of Biological Chemistry* **283**:  
1079 7280–7292.
- 1080 Yoshimoto S, Okada E, Umemoto H, Tamura K, Uno Y, Nishida-Umehara C,  
1081 Matsuda Y, Takamatsu N, Shiba T, Ito M. 2008. A W-linked DM-domain gene,  
1082 *DM-W*, participates in primary ovary development in *Xenopus laevis*. *PNAS* **105**:  
1083 2469–2474.



- 1084 Zhang HH, Xie YC, Li HJ, Zhuo JC, Zhang CX. 2021. Pleiotropic roles of the  
1085 orthologue of the *Drosophila melanogaster Intersex* gene in the brown  
1086 planthopper. *Genes* **12**: 379.
- 1087 Zhuo JC, Hu QL, Zhang HH, Zhang MQ, Jo SB, Zhang CX. 2018. Identification and  
1088 functional analysis of the doublesex gene in the sexual development of a  
1089 hemimetabolous insect, the brown planthopper. *Insect Biochemistry and Molecular*  
1090 *Biology* **102**: 31–42.
- 1091

1092 **Video**

1093 **Video 1. Time-lapse imaging of molting of *Thermobia domestica*.**

1094

1095 **Tables**

1096 **Table 1. Taxa and proteins used for molecular phylogenetic analysis of DMRT**

1097 **family.**

OTU name	gene	accession number	species	Order	Class/Subphylum	genome region	genome resource
Aasp_Dsx-like	<i>dsx</i> -like	GAZQ02010078.1	<i>Aretaon asperimus</i>	Phasmatodea	Ectognatha/Hexapoda		
Afra_Dsx3	<i>dsx</i> 3	AWC26109.1	<i>Artemia franciscana</i>	Anostraca	Brachiopoda/Crustacea		
Afra_Dsx4	<i>dsx</i> 4	AWC26111.1	<i>Artemia franciscana</i>	Anostraca	Brachiopoda/Crustacea		
Annu_Dmrt99B	<i>dmrt9</i> 9B	GATX01081132.1	<i>Annulipalpia</i> sp.	Trichoptera	Ectognatha/Hexapoda		
Annu_Dsx	<i>dsx</i>	GATX01084595.1	<i>Annulipalpia</i> sp.	Trichoptera	Ectognatha/Hexapoda		
Aros_Dsx	<i>dsx</i>	XP_012262263.1	<i>Athalia rosae</i>	Hymenoptera	Ectognatha/Hexapoda		
Baet_Dsx-like	<i>dsx</i> -like	GATU02014641.1	<i>Baetis</i> sp.	Ephemeroptera	Ectognatha/Hexapoda		
Bdor_Dsx	<i>dsx</i>	AAB99948.1	<i>Bactrocera dorsalis</i>	Diptera	Ectognatha/Hexapoda		
Bger_Dsx	<i>dsx</i>	PSN43312.1	<i>Blattella germanica</i>	Dictyoptera	Ectognatha/Hexapoda		
Bhye_Dsx	<i>dsx</i>	GAYK02032082.1	<i>Boreus hyemalis</i>	Mecoptera	Ectognatha/Hexapoda		
Bmor_Dmrt11E	<i>dmrt1</i> 1E	XP_004930266.1	<i>Bombyx mori</i>	Lepidoptera	Ectognatha/Hexapoda		
Bmor_Dmrt93B	<i>dmrt9</i> 3B	XP_004932028.3	<i>Bombyx mori</i>	Lepidoptera	Ectognatha/Hexapoda		
Bmor_Dmrt99B	<i>dmrt9</i> 9B	XP_004924389.2	<i>Bombyx mori</i>	Lepidoptera	Ectognatha/Hexapoda		
Bmor_Dsx	<i>dsx</i>	XP_012544211.1	<i>Bombyx mori</i>	Lepidoptera	Ectognatha/Hexapoda		
Bmut_Dmrt1	<i>dmrt1</i>	ELR53308.1	<i>Bos mutus</i>	Cetartiodactyla	Mammalia/Vertebrata		
Btau_Dmrt2	<i>dmrt2</i>	XP_005210039.1	<i>Bos taurus</i>	Cetartiodactyla	Mammalia/Vertebrata		
Btry_Dsx	<i>dsx</i>	AAV85890.1	<i>Bactrocera tryoni</i>	Diptera	Ectognatha/Hexapoda		
Caqu_Dsx	<i>dsx</i>	CAQU003748-RA	<i>Catajapyx aquilonaris</i>	Diplura	Entognatha/Hexapoda		
Ccap_Dsx	<i>dsx</i>	XP_012158607.1	<i>Ceratitis capitata</i>	Diptera	Entognatha/Hexapoda		
Ccor_Dsx	<i>dsx</i>	GATG02018436.1	<i>Corydalus cornutus</i>	Megaloptera	Ectognatha/Hexapoda		
Ceut_Dmrt11E	<i>dmrt1</i> 1E	GAUX02031275.1	<i>Ceuthophilus</i> sp.	Orthoptera	Ectognatha/Hexapoda		
Cfel_Dsx	<i>dsx</i>	GAYP02016500.1	<i>Ctenocephalides felis</i>	Siphonaptera	Ectognatha/Hexapoda		
Cgal_Dsx	<i>dsx</i>	GAWK02011923.1	<i>Ceratophyllus gallinae</i>	Siphonaptera	Ectognatha/Hexapoda		
Choo_Dmrt11E	<i>dmrt1</i> 1E	NQII01002646.1	<i>Clitarchus hookeri</i>	Phasmatodea	Ectognatha/Hexapoda		
Choo_Dsx-like	<i>dsx</i> -like	NQII01000109.1	<i>Clitarchus hookeri</i>	Phasmatodea	Ectognatha/Hexapoda		
Dcar_Dsx1	<i>dsx</i> 1	AIL86779.1	<i>Daphnia carina</i>	Diplostroca	Brachiopoda/Crustacea		
Dcar_Dsx2	<i>dsx</i> 2	AIL86780.1	<i>Daphnia carina</i>	Diplostroca	Brachiopoda/Crustacea		
Dgal_Dsx1	<i>dsx</i> 1	BAM33609.1	<i>Daphnia galeata</i>	Diplostroca	Brachiopoda/Crustacea		
Dgal_Dsx2	<i>dsx</i> 2	BAM33610.1	<i>Daphnia galeata</i>	Diplostroca	Brachiopoda/Crustacea		
Dmag_Dmrt11E	<i>dmrt1</i> 1e	BAG12871.1	<i>Daphnia magna</i>	Diplostroca	Brachiopoda/Crustacea		

Dmag_Dmrt93B	dm rt9 3b	BAG12872.1	<i>Daphnia magna</i>	Diplostroca	Brachiopoda /Crustacea		
Dmag_Dmrt99B	dm rt9 9b	BAG12873.1	<i>Daphnia magna</i>	Diplostroca	Brachiopoda /Crustacea		
Dmag_Dsx1	dsx 1	BAJ78307.1	<i>Daphnia magna</i>	Diplostroca	Brachiopoda /Crustacea		
Dmag_Dsx2	dsx 2	BAJ78309.1	<i>Daphnia magna</i>	Diplostroca	Brachiopoda /Crustacea		
Dmel_Dmrt11E	dm rt1 1e	NP_511146.2	<i>Drosophila melanogaster</i>	Diptera	Ectognatha/Hexapoda		
Dmel_Dmrt93B	dm rt9 3b	NP_524428.1	<i>Drosophila melanogaster</i>	Diptera	Ectognatha/Hexapoda		
Dmel_Dmrt99B	dm rt9 9b	NP_524549.1	<i>Drosophila melanogaster</i>	Diptera	Ectognatha/Hexapoda		
Dmel_Dsx	dsx	NP_731197.1	<i>Drosophila melanogaster</i>	Diptera	Ectognatha/Hexapoda		
Dpul_Dsx1	dsx 1	AGJ52190.1	<i>Daphnia pulex</i>	Diplostroca	Brachiopoda /Crustacea		
Dpul_Dsx2	dsx 2	BAM33608.1	<i>Daphnia pulex</i>	Diplostroca	Brachiopoda /Crustacea		
Drer_Dmrt1	dm rt1	AAQ04555.1	<i>Danio rerio</i>	Cypriniformes	Actinopterygii/Vertebrata		
Drer_Dmrt2	dm rt2	NP_571027.1	<i>Danio rerio</i>	Cypriniformes	Actinopterygii/Vertebrata		
Edan_dmrt11E	dm rt1 1E	EDAN008414-RA	<i>Ephemera danica</i>	Ephemeroptera	Ectognatha/Hexapoda		
Edan_dmrt93B	dm rt9 3B	EDAN004527-RA	<i>Ephemera danica</i>	Ephemeroptera	Ectognatha/Hexapoda		
Edan_dmrt99B	dm rt9 9B	EDAN010669-RA	<i>Ephemera danica</i>	Ephemeroptera	Ectognatha/Hexapoda		
Edan_Dsx-like	dsx - like		<i>Ephemera danica</i>	Ephemeroptera	Ectognatha/Hexapoda	ephdan_Scaffold2_3	i5k
Eins_Dsx-like	dsx - like	GCCL01024227.1	<i>Ecdyonurus insignis</i>	Ephemeroptera	Ectognatha/Hexapoda		
Enos_Dsx	dsx	GAXW02019001.1	<i>Euroleon nostras</i>	Neuroptera	Ectognatha/Hexapoda		
Epen_Dsx	dsx	GAWT02033840.1	<i>Empusa pennata</i>	Mantodea	Ectognatha/Hexapoda		
Esup_Dsx	dsx	GAVW02000373.1	<i>Epiophlebia superstes</i>	Odonata	Ectognatha/Hexapoda		
Eury_Dmrt11E	dm rt1 1E	GAZG02011227.1	<i>Eurylophella</i> sp.	Ephemeroptera	Ectognatha/Hexapoda		
Eury_Dsx-like	dsx - like	GAZG02000044.1	<i>Eurylophella</i> sp.	Ephemeroptera	Ectognatha/Hexapoda		
Focc_Dsx	dsx	FOCC007514-RA	<i>Frankliniella occidentalis</i>	Thysanoptera	Ectognatha/Hexapoda		
Gcor_Dsx	dsx	BAW32683.1	<i>Gnatocerus cornutus</i>	Coleoptera	Ectognatha/Hexapoda		
Harm_Dsx	dsx	XP_021192052.1	<i>Helicoverpa armigera</i>	Lepidoptera	Ectognatha/Hexapoda		
Hdeu_Dsx	dsx	maker-scaffold37size976698-augustus-gene-4.5-mRNA-1	<i>Holacanthella duospinosa</i>	Collembola	Entognatha/Hexapoda		i5k
Hydr_Dsx	dsx	GAVM02014074.1	<i>Hydroptila</i> sp.	Trichoptera	Ectognatha/Hexapoda		
Ibic_Dsx-like	dsx - like	GAXA02007870.1	<i>Isonychia bicolor</i>	Ephemeroptera	Ectognatha/Hexapoda		
Icra_Dsx	dsx	GAZH02011000.1	<i>Inocellia crassicornis</i>	Raphidioptera	Ectognatha/Hexapoda		
Lcup_Dmrt11E	dm rt1 1E	XP_023291847.1	<i>Lucilia cuprina</i>	Diptera	Ectognatha/Hexapoda		i5k
Lcup_Dmrt93B	dm rt9 3B	XP_023302612.1	<i>Lucilia cuprina</i>	Diptera	Ectognatha/Hexapoda		
Lcup_Dmrt99B	dm rt9 9B	XP_023308885.1	<i>Lucilia cuprina</i>	Diptera	Ectognatha/Hexapoda		
Lcup_Dsx	dsx	ADG37648.1	<i>Lucilia cuprina</i>	Diptera	Ectognatha/Hexapoda		
Lful_Dsx	dsx	LFUL018497-RA	<i>Ladona fulva</i>	Odonata	Ectognatha/Hexapoda		

Lmig_Dsx	dsx		<i>Locusta migratoria</i>	Orthoptera	Ectognatha/Hexapoda	scaffold3427	NCBI
Mdom_Dmrt11E	dmrt1E	XP_019890834.1	<i>Musca domestica</i>	Diptera	Ectognatha/Hexapoda		
Mdom_Dmrt99B	dmrt99B	XP_005186857.1	<i>Musca domestica</i>	Diptera	Ectognatha/Hexapoda		
Mdom_Dsx	dsx	AAR23813.1	<i>Musca domestica</i>	Diptera	Ectognatha/Hexapoda		
Mext_Dmrt99B	dmrt99B	Medex_00095964-RA	<i>Medauroidea extradentata</i>	Phasmatodea	Ectognatha/Hexapoda		
Mext_Dsx	dsx		<i>Medauroidea extradentata</i>	Phasmatodea	Ectognatha/Hexapoda	PNEQ01023967.1 [32614-32324]	i5k
Mext_Dsx-like	dsx-like	Medex_00099178-RA	<i>Medauroidea extradentata</i>	Phasmatodea	Ectognatha/Hexapoda	PNEQ01097711.1 [2988-3275]	i5k
Mfas_Dsx	dsx	GCNI01018035.1	<i>Meroplius fasciculatus</i>	Diptera	Ectognatha/Hexapoda		
Mmac_Dsx	dsx	BAM33613.1	<i>Moina macrochaeta</i>	Diplostroca	Brachiopoda/Crustacea		
Mmus_Dmrt1	dmrt1	AAO41736.1	<i>Mus musculus</i>	Rodentia	Mammalia/Vertebrata		
Mrel_Dsx	dsx	GASW02021994.1	<i>Mantis religiosa</i>	Mantodea	Ectognatha/Hexapoda		
Mviol_Dsx	dsx	GATA02010186.1	<i>Meloe violaceus</i>	Coleoptera	Ectognatha/Hexapoda		
Ofur_Dsx	dsx	AHF81635.1	<i>Ostrinia furnacalis</i>	Lepidoptera	Ectognatha/Hexapoda		i5k
Otau_Dsx	dsx	AEX92938.1	<i>Onthophagus taurus</i>	Coleoptera	Ectognatha/Hexapoda		
Ppra_Dsx	dsx	GAVV02027199.1	<i>Pseudomallada prasina</i>	Neuroptera	Ectognatha/Hexapoda		
Psch_Dsx-like	dsx-like	GAWJ02028457.1	<i>Peruphasma schultzei</i>	Phasmatodea	Ectognatha/Hexapoda		i5k
Smag_Dmrt99B	dmrt99B	GEYQ01032489.1	<i>Steganacarus magnus</i>	Oribatida	Arachnida/Chelicerata		
Tcas_Dmrt93B	dmrt93B	XP_008199135.1	<i>Tribolium castaneum</i>	Coleoptera	Ectognatha/Hexapoda		
Tcas_Dmrt99B	dmrt99B	XP_975675.1	<i>Tribolium castaneum</i>	Coleoptera	Ectognatha/Hexapoda		
Tcas_Dsx	dsx	NP_001345539.1	<i>Tribolium castaneum</i>	Coleoptera	Ectognatha/Hexapoda		
Tcri_Dsx-like	dsx-like	GAVX02010884.1	<i>Timema cristinae</i>	Phasmatodea	Ectognatha/Hexapoda		
Tdic_Dsx	dsx	BAM93340.1	<i>Trypoxylus dichotomus</i>	Coleoptera	Ectognatha/Hexapoda		
Tdom_Dmrt11E	dmrt11E	this study	<i>Thermobia domestica</i>	Zygentoma	Ectognatha/Hexapoda	scaffold42162_cov39 [159031-158906]	
Tdom_Dmrt93B	dmrt93B	this study	<i>Thermobia domestica</i>	Zygentoma	Ectognatha/Hexapoda	scaffold1624327_cov47 [121390-121265]	
Tdom_Dmrt99B	dmrt99B	this study	<i>Thermobia domestica</i>	Zygentoma	Ectognatha/Hexapoda	scaffold21840_cov24 [214972-214787]	
Tdom_Dsx	dsx	this study	<i>Thermobia domestica</i>	Zygentoma	Ectognatha/Hexapoda		
Tdom_Dsx-like	dsx-like	this study	<i>Thermobia domestica</i>	Zygentoma	Ectognatha/Hexapoda	scaffold27567_cov49 [365805-281362]	
Tger_Dsx-like	dsx-like	GASO02037568.1	<i>Tricholepidion gertschi</i>	Zygentoma	Ectognatha/Hexapoda		
Tsub_Dsx	dsx	GASQ02027559.1	<i>Tetrix subulata</i>	Orthoptera	Ectognatha/Hexapoda		
Xant_Dsx	dsx	GAUI02048130.1	<i>Xanthostigma</i> sp.	Raphidioptera	Ectognatha/Hexapoda		
Xlae_Dmrt1	dmrt1	NP_001089969.1	<i>Xenopus laevis</i>	Anura	Amphibia/Vertebrata		
Xlae_Dmrt4	dmrt4	AAH70678.2	<i>Xenopus laevis</i>	Anura	Amphibia/Vertebrata		
Xlae_Dmrt5	dmrt5	AAI70166.1	<i>Xenopus laevis</i>	Anura	Amphibia/Vertebrata		

1099 **Table 2. Results of RT-qPCR assay and Brunner–Munzel test.** Significant levels are indicated by asterisks in significance column: \* $P < 0.05$ ,  
 1100 \*\* $P < 0.01$ , \*\*\* $P < 0.001$ . n.s. means non-significance.

experiment	treatment	sample size (N)	median		proportion of $2^{-\Delta Ct}$	95% confidence interval		Brunner-Munzel test			P-value adjusted by Holm's method	significance	graph #
			$\Delta Ct$	$2^{-\Delta Ct}$		statistics	df	P-value					
<i>dsx</i> male-type expression level	male	12	8.59	2.66.E-03	1.00								
	female	8	13.89	6.64.E-05	0.02	0.83	1.07	8.25	12.82	1.75.E-06	-	***	Figure 1D
<i>dsx</i> female-type expression level	male	11	9.98	9.90.E-04	1.00								
	female	12	5.77	1.83.E-02	18.47	-0.01	0.01	-92.63	20.95	2.20.E-16	-	***	Figure 1D
<i>dsx-like</i> expression level	male	12	3.62	8.13.E-02	1.00								
	female	12	4.71	3.83.E-02	0.47	0.58	1.02	2.86	21.84	9.24.E-03	-	**	Figure 1E
<i>dsx</i> expression level in males	<i>egfp</i>	12	7.50	5.52.E-03	1.00								
	<i>dsx</i> all	8	9.24	1.66.E-03	0.30	0.45	1.03	1.78	13.61	9.68.E-02	1.94.E-01	n.s.	Figure 1–figure supplement 3B
	<i>dsx-like</i>	10	7.14	7.10.E-03	1.29	0.07	0.57	-1.54	17.40	1.43.E-01	1.43.E-01	n.s.	
<i>dsx</i> expression level in males excluding outliers	<i>egfp</i>	12	7.50	5.52.E-03	1.00								
	<i>dsx</i> all	7	9.32	1.57.E-03	0.28	0.64	1.05	3.64	13.87	2.73.E-03	5.45.E-03	**	Figure 1–figure supplement 3A
	<i>dsx-like</i>	10	7.14	7.10.E-03	1.29	0.07	0.57	-1.54	17.40	1.43.E-01	1.43.E-01	n.s.	
<i>dsx</i> expression level in females	<i>egfp</i>	10	5.18	2.76.E-02	1.00								
	<i>dsx</i> all	17	6.23	1.33.E-02	0.48	0.57	0.99	2.78	16.21	1.33.E-02	2.65.E-02	*	Figure 1–figure supplement 3A
	<i>dsx-like</i>	9	5.17	2.78.E-02	1.01	0.20	0.82	0.08	15.38	9.40.E-01	9.40.E-01	n.s.	
<i>dsx-like</i> expression level in males	<i>egfp</i>	12	5.72	1.95.E-02	1.00								
	<i>dsx</i> all	8	6.17	1.39.E-02	0.72	0.50	0.98	2.08	17.99	5.19.E-02	5.19.E-02	n.s.	Figure 1–figure supplement 3A
	<i>dsx-like</i>	10	10.17	8.68.E-04	0.04	1.00	1.00	Inf	NaN	2.20.E-16	4.40.E-16	***	
<i>dsx-like</i> expression level in females	<i>egfp</i>	10	6.08	1.49.E-02	1.00								
	<i>dsx</i> all	17	6.31	1.26.E-02	0.85	0.47	0.93	1.82	16.18	8.76.E-02	8.76.E-02	n.s.	Figure 1–figure supplement 3A
	<i>dsx-like</i>	9	11.58	3.27.E-04	0.02	1.00	1.00	Inf	NaN	2.20.E-16	4.40.E-16	***	

	<i>egfp</i>	5	15.00	3.06.E-05	1.00									
vitellogenin-1 expression level in males	<i>dsx</i> all	9	4.42	4.68.E-02	1530.72	-0.05	0.09	-15.20	10.67	1.44.E-08	2.87.E-08	***	Figure 4D	
	<i>dsx-like</i>	7	10.18	8.62.E-04	28.18	-0.12	0.41	-3.09	8.42	1.39.E-02	1.39.E-02	*		
	<i>dsx+dsx-like</i>	9	4.28	5.14.E-02	1678.94	0.00	0.00	-Inf	NaN	2.20.E-16	6.60.E-16	***		
	<i>egfp</i>	3	16.76	9.01.E-06	1.00									
vitellogenin-2 expression level in males	<i>dsx</i> all	8	11.24	4.13.E-04	45.89	0.00	0.00	-Inf	NaN	2.20.E-16	6.60.E-16	***	Figure 4D	
	<i>dsx-like</i>	5	15.48	2.19.E-05	2.43	-0.24	0.51	-2.46	5.56	5.24.E-02	6.19.E-01	n.s.		
	<i>dsx+dsx-like</i>	8	10.64	6.27.E-04	28.64	0.00	0.00	-Inf	NaN	2.20.E-16	6.60.E-16	***		
	<i>egfp</i>	10	11.28	4.21.E-04	1.00									
vitellogenin-3 expression level in males	<i>dsx</i> all	10	3.25	1.07.E-01	254.99	-0.09	0.23	-6.00	9.86	1.40.E-04	2.80.E-04	***	Figure 4D	
	<i>dsx-like</i>	10	8.73	2.37.E-03	5.64	-0.03	0.39	-3.29	15.01	4.97.E-03	4.97.E-03	**		
	<i>dsx+dsx-like</i>	9	2.82	1.42.E-01	336.55	0.00	0.00	-Inf	NaN	2.20.E-16	6.60.E-16	***		
	<i>egfp</i>	8	-2.67	6.34.E+00	1.00									
vitellogenin-1 expression level in females	<i>dsx</i> all	10	-0.44	1.41.E+00	0.22	0.51	1.02	2.20	15.51	4.33.E-02	4.33.E-02	*	Figure 4E	
	<i>dsx-like</i>	7	-0.29	1.22.E-00	0.19	0.70	1.08	4.55	10.89	8.51.E-04	2.56.E-03	**		
	<i>dsx+dsx-like</i>	8	0.90	5.40.E-01	0.09	0.58	1.10	3.00	8.82	1.52.E-02	3.05.E-02	*		
	<i>egfp</i>	8	1.84	2.80.E-01	1.00									
vitellogenin-2 expression level in females	<i>dsx</i> all	10	4.34	4.96.E-02	0.18	0.65	1.05	3.68	15.57	2.11.E-03	4.22.E-03	**	Figure 4E	
	<i>dsx-like</i>	7	5.24	2.65.E-02	0.09	0.83	1.06	8.45	12.94	1.27.E-06	3.80.E-06	***		
	<i>dsx+dsx-like</i>	8	6.10	1.48.E-02	0.05	0.63	1.15	3.54	7.29	8.92.E-03	8.92.E-03	**		
	<i>egfp</i>	8	-3.37	1.03.E+01	1.00									
vitellogenin-3 expression level in females	<i>dsx</i> all	10	-1.98	3.95.E+00	0.38	0.65	1.07	3.75	11.23	3.12.E-03	6.23.E-03	**	Figure 4E	
	<i>dsx-like</i>	8	0.84	7.82.E-01	0.08	0.81	1.06	7.56	12.60	4.98.E-06	1.49.E-05	***		
	<i>dsx+dsx-like</i>	8	0.05	1.09.E+00	0.11	0.57	1.13	2.95	7.56	1.97.E-02	1.97.E-02	*		

1101 The source data of this table can be obtained in the Table2–source data 1 file.

1102

1103 **Table 3. Results of Smirnov–Grubbs' test for expression level of *dsx* mRNA in nymphal RNAi males.** The determination of whether a value  
 1104 is an outlier or not is based on the *P*-value and is shown in the “outlier?” column.

<b>data</b>	<b>max/min</b>	<b>value</b>	<b>G</b>	<b>U</b>	<b>P-value</b>	<b>outlier?</b>
<i>egfp</i>	max	10.45	1.8587	0.65738	2.73.E-01	no
	min	5.31	1.59672	0.74715	5.74.E-01	no
<i>dsx</i>	max	10.47	0.97	0.85	1.00.E+00	no
	min	5.23	2.27	0.15688	5.14.E-03	yes
<i>dsx-like</i>	max	7.70	1.01	0.88	1.00.E+00	no
	min	5.12	2.08	0.47	8.35.E-02	no
reanalysis of <i>dsx</i>	max	10.47	1.52	0.55	3.52.E-01	no
	min	8.44	1.42	0.61	4.70.E-01	no

1105

1106



1107 **Table 4. Results of generalized linear model of female traits.** Significant levels are indicated by asterisks in significance column: \* $P < 0.05$ ,  
 1108 \*\* $P < 0.01$ , \*\*\* $P < 0.001$ . n.s. means non-significance.

objective variable	sample size (N)	explanatory variables	LR Chisq	Df	P-value	significance	Fig #
ovipositor length	<i>egfp</i> : 10, <i>dsx</i> all: 17, <i>dsx-like</i> : 9, <i>dsx+dsx-like</i> : 12, total: 48	<i>dsx</i> RNAi	0.26	1	6.08.E-01	n.s.	Figure 2H
		<i>dsx-like</i> RNAi	0.58	1	4.47.E-01	n.s.	
		prothoracic width	297.00	1	2.00.E-16	***	
		<i>dsx</i> RNAi: <i>dsx-like</i> RNAi	2.67	1	1.02.E-01	n.s.	
ovipositor length	<i>egfp</i> : 8, <i>dsx</i> all: 8, <i>dsx</i> male-type: 7, <i>dsx</i> female-type: 13, total: 36	<i>dsx</i> all RNAi	1.29	1	2.56.E-01	n.s.	Figure 2–figure supplement 3
		<i>dsx</i> male-type RNAi	1.29	1	2.56.E-01	n.s.	
		<i>dsx</i> female-type RNAi	0.42	1	5.18.E-01	n.s.	
		prothoracic width	146.52	1	2.00.E-16	***	
prothoracic width	<i>egfp</i> : 10, <i>dsx</i> all: 17, <i>dsx-like</i> : 9, <i>dsx+dsx-like</i> : 13, total: 49	<i>dsx</i> RNAi	2.17	1	1.41.E-01	n.s.	Figure 2–figure supplement 4
		<i>dsx-like</i> RNAi	1.96	1	1.61.E-01	n.s.	
		<i>dsx</i> RNAi: <i>dsx-like</i> RNAi	2.16	1	1.41.E-01	n.s.	
previtellogenic oocyte number	<i>egfp</i> : 7, <i>dsx</i> all: 16, <i>dsx-like</i> : 10, <i>dsx+dsx-like</i> : 9, total: 42	<i>dsx</i> RNAi	0.08	1	7.83.E-01	n.s.	Figure 3D
		<i>dsx-like</i> RNAi	0.23	1	6.31.E-01	n.s.	
		prothoracic width	0.97	1	3.25.E-01	n.s.	

		<i>dsx</i> RNAi: <i>dsx-like</i> RNAi	0.06	1	8.10.E-01	n.s.	
early vitellogenic oocyte number	<i>egfp</i> : 7, <i>dsx</i> all: 16, <i>dsx-like</i> : 10, <i>dsx+dsx-like</i> : 9, total: 42	<i>dsx</i> RNAi	0.11	1	7.45.E-01	n.s.	Figure 3D
		<i>dsx-like</i> RNAi	0.08	1	7.77.E-01	n.s.	
		prothoracic width	3.50	1	6.14.E-02	n.s.	
		<i>dsx</i> RNAi: <i>dsx-like</i> RNAi	0.62	1	4.30.E-01	n.s.	
late vitellogenic oocyte number	<i>egfp</i> : 7, <i>dsx</i> all: 16, <i>dsx-like</i> : 10, <i>dsx+dsx-like</i> : 9, total: 42	<i>dsx</i> RNAi	0.46	1	5.00.E-01	n.s.	Figure 3D
		<i>dsx-like</i> RNAi	1.12	1	2.90.E-01	n.s.	
		prothoracic width	9.84	1	1.71.E-03	**	
		<i>dsx</i> RNAi: <i>dsx-like</i> RNAi	2.16	1	1.42.E-01	n.s.	
oocyte size	<i>egfp</i> : 5, <i>dsx</i> all: 9, <i>dsx-like</i> : 7, <i>dsx+dsx-like</i> : 2, total: 23	<i>dsx</i> RNAi	0.1689	1	6.81.E-01	n.s.	Figure3–figure supplement 3
		<i>dsx-like</i> RNAi	3.4291	1	6.41.E-02	n.s.	
		prothoracic width	4.273	1	3.87.E-02	*	
		<i>dsx</i> RNAi: <i>dsx-like</i> RNAi	1.4509	1	2.23.E-01	n.s.	

1109 The source data of this table can be obtained in the Table4–source data 1 file.

1110

1111 **Table 5. Results of generalized linear model of male traits.** *P*-values are indicated by asterisks in significance column: \*\**P* < 0.01. n.s. means  
 1112 non-significance.

objective variable	sample size ( <i>N</i> )	explanatory variables	LR Chisq	Df	<i>P</i> -value	significance	Fig #
sperm number	<i>egfp</i> : 9 <i>dsx</i> all: 6 <i>dsx-like</i> : 10 <i>dsx+dsx-like</i> : 4, total: 29	<i>dsx</i> RNAi	7.93	1	4.87.E-03	**	Figure 3C
		<i>dsx-like</i> RNAi	2.06	1	1.51.E-01	n.s.	
		prothoracic width	8.68	1	3.21.E-03	**	
		<i>dsx</i> RNAi: <i>dsx-like</i> RNAi	0.02	1	8.79.E-01	n.s.	
prothoracic width	<i>egfp</i> : 12, <i>dsx</i> all: 8, <i>dsx-like</i> : 10, <i>dsx+dsx-like</i> : 6, total: 36	<i>dsx</i> RNAi	0.03	1	8.71.E-01	n.s.	Figure 2–figure supplement 4
		<i>dsx-like</i> RNAi	2.82	1	9.31.E-02	n.s.	
		<i>dsx</i> RNAi: <i>dsx-like</i> RNAi	1.09	1	2.96.E-01	n.s.	

1113 The source data of this table can be obtained in the Table5–source data 1 file.

1114

1115 **Table 6. Primers' list used in this study.**

No.	expeiment	target	primer name	primer sequence (5' to 3')	length	note
1	5' RACE	<i>doublesex (dsx)</i>	Tdom_ <i>dsx</i> _RACE_01	TCGCGTGACAAGGAAGAAGGCCCCCGG	26	gene specific primer
2	5' RACE	<i>dsx</i>	Tdom_ <i>dsx</i> _RACE_02	AGGCCCCGGAATTGAAGAAGCACCT	25	nested gene specific primer
3	5' RACE	<i>doublesex-like (dsx-like)</i>	Tdom_ <i>dsx-like</i> _RACE_01	CAC TTTGAAAACGCAGGGCTGGATG	25	gene specific primer
4	5' RACE	<i>dsx-like</i>	Tdom_ <i>dsx-like</i> _RACE_02	GGGCTGGATGTTCTGCTGTAGTTGAA	25	nested gene specific primer
5	3' RACE	<i>dsx</i>	Tdom_ <i>dsx</i> _RACE_03	GCTTCTTCAATTCCGGGGCCTTCTTCC	27	gene specific primer
6	3' RACE	<i>dsx</i>	Tdom_ <i>dsx</i> _RACE_04	TCAATTCCGGGGCCTTCTTCTTGTC	27	nested gene specific primer
7	3' RACE	<i>dsx-like</i>	Tdom_ <i>dsx-like</i> _RACE_03	AGACAGCAGCCAAATGACGTCAAGA	25	gene specific primer
8	3' RACE	<i>dsx-like</i>	Tdom_ <i>dsx-like</i> _RACE_04	ACAGCAGCCAAATGACGTCAAGAGA	25	nested gene specific primer
9	RT-qPCR	<i>ribosomal protein 49 (rp49)</i>	Tdom_ <i>rp49</i> _RT-qPCR_F	ACCCACCATAGTCAAGAAGCGGA	23	reference gene
10	RT-qPCR	<i>ribosomal protein 49 (rp49)</i>	Tdom_ <i>rp49</i> _RT-qPCR_R	AACTGTCCCTTAAACCGCCTTCG	23	reference gene
11	RT-qPCR	<i>dsx</i> male-specific region	Tdom_ <i>dsx</i> _male_RT-qPCR_F	GCTACCGCTTGAAACATTGCCTT	23	
12	RT-qPCR	<i>dsx</i> male-specific region	Tdom_ <i>dsx</i> _male_RT-qPCR_R	AGTGCCATGGATCGTAATTCTGCT	24	
13	RT-qPCR	<i>dsx</i> female-specific region	Tdom_ <i>dsx</i> _female_RT-qPCR_F	CTACCGCTTGAAACATTGCCTTT	23	
14	RT-qPCR	<i>dsx</i> female-specific region	Tdom_ <i>dsx</i> _female_RT-qPCR_R	TGCCCTGATTCATGCATTGA	20	
15	RT-qPCR	<i>dsx</i> common region	Tdom_ <i>dsx</i> _RT-qPCR_F	ACCCAGCCATGCCTCCTAATGTA	23	
16	RT-qPCR	<i>dsx</i> common region	Tdom_ <i>dsx</i> _RT-qPCR_R	CTTCGAGCGTCCATCAGAACGAC	23	
17	RT-qPCR	<i>dsx-like</i>	Tdom_ <i>dsx-like</i> _RT-qPCR_F	ACGGGTTGTTGCTTTACATCTGT	23	
18	RT-qPCR	<i>dsx-like</i>	Tdom_ <i>dsx-like</i> _RT-qPCR_R	TCTCTTGACGTCATTTGGCTGCT	23	
19	RT-qPCR	<i>vitellogenin-1</i>	Tdom_ <i>vitellogenin-1</i> _RT-qPCR_F	TGCTCCATTCAACAACCAGC	20	

20	RT-qPCR	<i>vitellogenin-1</i>	Tdom_ <i>vitellogenin-1</i> _RT-qPCR_R	AGCCCAGATGAACTTGACGA	20	
21	RT-qPCR	<i>vitellogenin-2</i>	Tdom_ <i>vitellogenin-2</i> _RT-qPCR_F	CCAGTGATGGTGGCAATTCAGGA	23	
22	RT-qPCR	<i>vitellogenin-2</i>	Tdom_ <i>vitellogenin-2</i> _RT-qPCR_R	TGTGGCTGTGACTGTCGTTTTGT	23	
23	RT-qPCR	<i>vitellogenin-3</i>	Tdom_ <i>vitellogenin-3</i> _RT-qPCR_F	CACCAGCGATGTTGACGAGAAGA	23	
24	RT-qPCR	<i>vitellogenin-3</i>	Tdom_ <i>vitellogenin-3</i> _RT-qPCR_R	GCTCAAACCTCAGGCTCAAGTGGGA	23	
25	dsRNA	<i>egfp</i>	<i>egfp</i> _dsRNA_F	ATCATGGCCGACAAGCAGAA	20	control of RNAi assay
26	dsRNA	<i>egfp</i>	<i>egfp</i> _dsRNA_R	AACTCCAGCAGGACCATGTG	20	control of RNAi assay
29	dsRNA	<i>dsx</i> common region	Tdom_ <i>dsx</i> _dsRNA_F	CCAAGCCCAAGACGAAGC	18	
30	dsRNA	<i>dsx</i> common region	Tdom_ <i>dsx</i> _dsRNA_R	CCGACTGTTACATTAGGAGGC	21	
31	dsRNA	<i>dsx</i> male-specific region	Tdom_ <i>dsx</i> _male-type_dsRNA_F	GCAGAATTACGATCCATGGCAC	22	
32	dsRNA	<i>dsx</i> male-specific region	Tdom_ <i>dsx</i> _male-type_dsRNA_R	CGTACTGGCCCTTTACATGGT	21	
33	dsRNA	<i>dsx</i> female-specific region	Tdom_ <i>dsx</i> _female-type_dsRNA_F	TGCATGAATCAGGGCATTATTG	22	
34	dsRNA	<i>dsx</i> female-specific region	Tdom_ <i>dsx</i> _female-type_dsRNA_R	TCAATTGATCTGACTTGTGCCT	22	
35	dsRNA	<i>dsx-like</i>	Tdom_ <i>dsx-like</i> _dsRNA_F	CTCATGTGCAGTGATGTGGC	20	
36	dsRNA	<i>dsx-like</i>	Tdom_ <i>dsx-like</i> _dsRNA_R	TGCGTCAATGAACAGCGAAA	20	
37	dsRNA	pCR4-TOPO vector	T7-pCR4-TOPO_F	taatacgactcactatagggAGACCACGTCCTGCAGGTTTAAACG	45	T7 flanked
38	dsRNA	pCR4-TOPO vector	T7-pCR4-TOPO_R	taatacgactcactatagggAGACCACCGAATTGAATTTAGCGGC	45	T7 flanked

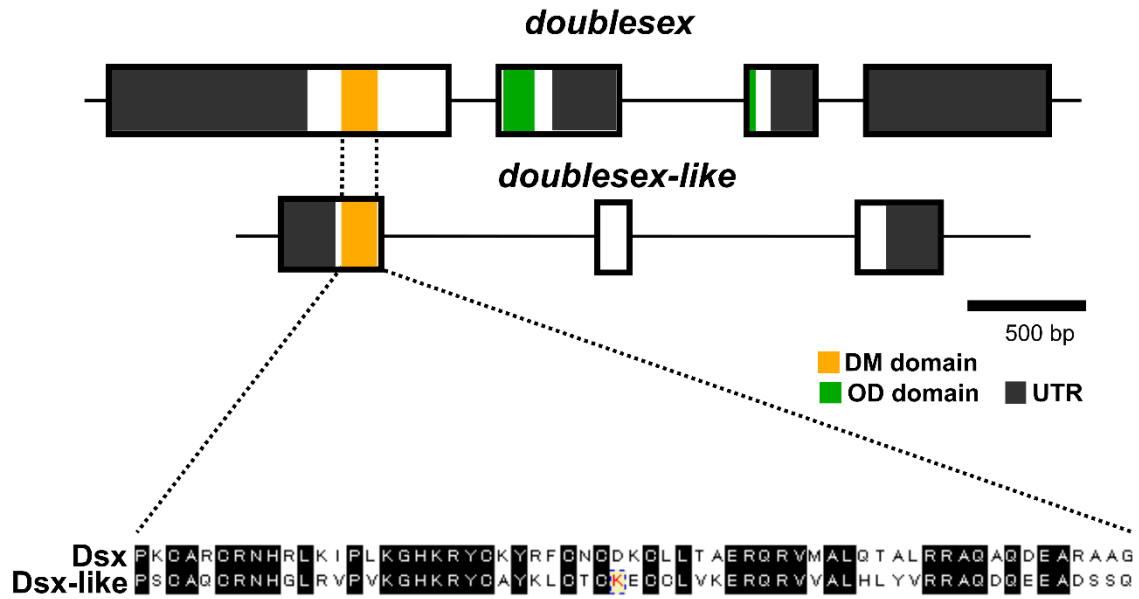
1116

## 1117 Figure Supplements

```
Aasp_Dsx-like 1 NSMNRLLCALCRNHLKIPVKGHKRFYVGLCLCKECLVKEQRVVMHLYFRRQQEEDRGS 65
Afra_Dsx3 1 RTRVPTCARCRNHGKIITLGRHKRYCQFRACSKLCVLTVDQKRVMAAQVALRRQAQDEENGVF 65
Afra_Dsx4 1 KMRMPTCARCRNHGQVVKLRGKRYCFSRHLCDRCALSTSEQRVMAAQVALRRQAQDEENGIV 65
Annu_Dmrt99B 1 YQRTFKCARCRNHGVSALKGKRYCRWRDVCACAKCTLIAERQVMAAQVALRRQAQDEENGSE 65
Annu_Dsx 1 PRTPFNCARCRNHLKIALKGHKRYCYVYCNCDKCLTAERQVMAAQVALRRQAQDEENGSE 65
Aros_Dsx 1 PRTPFNCARCRNHLKIALKGHKRYCYVYCNCEKCLTAERQVMAAQVALRRQAQDEENGSE 65
Baet_Dsx 1 ALSNRMCAQCNHGLKIPVKGHKRYCFLVLCNQCCLVKEQRVVMHLYFRRQQEEDAEAEA 65
Bdor_Dsx 1 PRTPFNCARCRNHLKIALKGHKRYCFFRCTCEKCLTAERQVMAAQVALRRQAQDEENGSE 65
Bqer_Dsx 1 PRTPFNCARCRNHLKIALKGHKRYCFFRCTCEKCLTAERQVMAAQVALRRQAQDEENGSE 65
Bhye_Dsx 1 PRTPFNCARCRNHLKIALKGHKRYCFRNCNYCYKILTAERQVMAAQVALRRQAQDEENGSE 65
Bmor_Dmrt11E 1 ALRTPFKCARCRNHGVSCLKGHKRCLRWREDCRCPGCLLVLRQVMAAQVALRRQAQDEENGSE 65
Bmor_Dmrt93B 1 RARVFKCARCRNHGLISLKGHKACAYRHCQCFKCGLKERQVMAAQVALRRQAQDEENGSE 65
Bmor_Dmrt99B 1 YQRTFKCARCRNHGVSALKGKRYCRWRDVCACAKCTLIAERQVMAAQVALRRQAQDEENGSE 65
Bmor_Dsx 1 PRAPFNCARCRNHLKIALKGHKRYCYVYCNCEKCLTAERQVMAAQVALRRQAQDEENGSE 65
Bmut_Dmrt1 1 SPLRFKCARCRNHGVSPLKGHKRYCFWRDCCQCKNCLIAERQVMAAQVALRRQAQDEENGSE 65
Btau_Dmrt2 1 LSRTPFKCARCRNHGVSCLKGHKRYCRWRDCCQCANCLLVLRQVMAAQVALRRQAQDEENGSE 65
Btry_Dsx 1 PRTPFNCARCRNHLKIALKGHKRYCFFRCTCEKCLTAERQVMAAQVALRRQAQDEENGSE 65
Cacu_Dsx 1 NSRTPFKCARCRNHGLIATVKGHKRYCYVYCNCEKCLTAERQVMAAQVALRRQAQDEENGSE 65
Ccap_Dsx 1 PRTPFNCARCRNHLKIALKGHKRYCFFRCTCEKCLTAERQVMAAQVALRRQAQDEENGSE 65
Ccor_Dsx 1 PRTPFNCARCRNHLKIALKGHKRYCYVYCNCEKCLTAERQVMAAQVALRRQAQDEENGSE 65
Ceut_Dmrt11E 1 LLRTFKCARCRNHGVSCLKGHKRCLRWREDCRCPGCLLVLRQVMAAQVALRRQAQDEENGSE 65
Cfel_Dsx 1 PRTPFNCARCRNHLKIALKGHKRYCYVYCNCEKCLTAERQVMAAQVALRRQAQDEENGSE 65
Cgal_Dsx 1 PRTPFNCARCRNHLKIALKGHKRYCYVYCNCEKCLTAERQVMAAQVALRRQAQDEENGSE 65
Choo_Dmrt11E 1 LLRTFKCARCRNHGVSCLKGHKRCLRWREDCRCPGCLLVLRQVMAAQVALRRQAQDEENGSE 65
Choo_Dsx-like 1 NSINRLCALCRNHLKIPVKGHKRYCYVYCNCEKCLVKEQRVVMHLYFRRQQEEDRGS 65
Dcar_Dsx1 1 SQRHPTCALCRNHQITITLKGHKRYCFFRCTCEKCLTAERQVMAAQVALRRQAQDEENGSE 65
Dcar_Dsx2 1 SCRNPFCALCRNHGINSPLKGHKRYCFFRCTCEKCLTAERQVMAAQVALRRQAQDEENGSE 65
Dgal_Dsx1 1 TORHPTCALCRNHQITITLKGHKRYCFFRCTCEKCLTAERQVMAAQVALRRQAQDEENGSE 65
Dgal_Dsx2 1 SCRNPFCALCRNHGINSPLKGHKRYCFFRCTCEKCLTAERQVMAAQVALRRQAQDEENGSE 65
Dmag_Dmrt11E 1 LLRTFKCARCRNHGVSCLKGHKRCLRWREDCRCPGCLLVLRQVMAAQVALRRQAQDEENGSE 65
Dmag_Dmrt93B 1 ALRPFKCARCRNHGVSILKGHKRCHRFKDCCLVKNCLIAERQVMAAQVALRRQAQDEENGSE 65
Dmag_Dmrt99B 1 YQRTFKCARCRNHGVSALKGKRYCRWRDVCACAKCTLIAERQVMAAQVALRRQAQDEENGSE 65
Dmag_Dsx1 1 SQRHPTCALCRNHQITITLKGHKRYCFFRCTCEKCLTAERQVMAAQVALRRQAQDEENGSE 65
Dmag_Dsx2 1 SCRNPFCALCRNHGINSPLKGHKRYCFFRCTCEKCLTAERQVMAAQVALRRQAQDEENGSE 65
Dmel_Dmrt11E 1 LLRTFKCARCRNHGVSCLKGHKRCLRWREDCRCPGCLLVLRQVMAAQVALRRQAQDEENGSE 65
Dmel_Dmrt93B 1 TNRVFKCARCRNHGVSILKGHKRCLRWREDCRCPGCLLVLRQVMAAQVALRRQAQDEENGSE 65
Dmel_Dmrt99B 1 YQRTFKCARCRNHGVSALKGKRYCRWRDVCACAKCTLIAERQVMAAQVALRRQAQDEENGSE 65
Dmel_Dsx 1 PRTPFNCARCRNHLKIALKGHKRYCYVYCNCEKCLTAERQVMAAQVALRRQAQDEENGSE 65
Dpu1_Dsx1 1 TORHPTCALCRNHQITITLKGHKRYCFFRCTCEKCLTAERQVMAAQVALRRQAQDEENGSE 65
Dpu1_Dsx2 1 SCRNPFCALCRNHGINSPLKGHKRYCFFRCTCEKCLTAERQVMAAQVALRRQAQDEENGSE 65
Dzer_Dmrt1 1 PSRMFKCARCRNHGVSPLKGHKRYCFFRCTCEKCLTAERQVMAAQVALRRQAQDEENGSE 65
Dzer_Dmrt2 1 LSRTPFKCARCRNHGVSCLKGHKRCLRWREDCRCPGCLLVLRQVMAAQVALRRQAQDEENGSE 65
Edan_Dmrt93B 1 GARRFKCARCRNHGMIISLKGHKRCHRFKDCCLVKNCLIAERQVMAAQVALRRQAQDEENGSE 65
Edan_Dmrt11E 1 VLRTFKCARCRNHGVSILKGHKRCLRWREDCRCPGCLLVLRQVMAAQVALRRQAQDEENGSE 65
Edan_Dmrt99B 1 YQRTFKCARCRNHGVSALKGKRYCRWRDVCACAKCTLIAERQVMAAQVALRRQAQDEENGSE 65
Edan_Dsx-like 1 TSSNRLCAQRNHLRVPVGRHKRYCFFRCTCEKCLTAERQVMAAQVALRRQAQDEENGSE 65
Eins_Dsx-like 1 QGSNRLCAQRNHLRVPVGRHKRYCFFRCTCEKCLTAERQVMAAQVALRRQAQDEENGSE 65
Enos_Dsx 1 PRTPFNCARCRNHLKIALKGHKRYCYVYCNCEKCLTAERQVMAAQVALRRQAQDEENGSE 65
Epen_Dsx 1 PRTPFNCARCRNHLKIALKGHKRYCYVYCNCEKCLTAERQVMAAQVALRRQAQDEENGSE 65
Esup_Dsx 1 ARTPFKCARCRNHLKIALKGHKRYCYVYCNCEKCLTAERQVMAAQVALRRQAQDEENGSE 65
Eury_Dmrt11E 1 VLRSFKCARCRNHGVSILKGHKRCLRWREDCRCPGCLLVLRQVMAAQVALRRQAQDEENGSE 65
Eury_Dsx-like 1 KTASRLCAQRNHLKIPVKGHKRYCFFRCTCEKCLTAERQVMAAQVALRRQAQDEENGSE 65
Focc_Dsx 1 ARTPFKCALCRNHLKIALKGHKRYCYVYCNCEKCLTAERQVMAAQVALRRQAQDEENGSE 65
Geor_Dsx 1 PRTPFNCARCRNHLKIALKGHKRYCYVYCNCEKCLTAERQVMAAQVALRRQAQDEENGSE 65
Harm_Dsx 1 PRAPFNCARCRNHLKIALKGHKRYCYVYCNCEKCLTAERQVMAAQVALRRQAQDEENGSE 65
Hdeu_Dsx 1 SARTFKCARCRNHGVSALKGKRYCYVYCNCEKCLTAERQVMAAQVALRRQAQDEENGSE 65
Hydc_Dsx 1 PRTPFNCARCRNHLKIALKGHKRYCYVYCNCEKCLTAERQVMAAQVALRRQAQDEENGSE 65
IdiC_Dsx-like 1 QGSNRLCAQRNHLRVPVGRHKRYCFFRCTCEKCLTAERQVMAAQVALRRQAQDEENGSE 65
Iora_Dsx 1 PRTPFNCARCRNHLKIALKGHKRYCYVYCNCEKCLTAERQVMAAQVALRRQAQDEENGSE 65
Lcup_Dmrt11E 1 MLRTPFKCARCRNHGVSILKGHKRCLRWREDCRCPGCLLVLRQVMAAQVALRRQAQDEENGSE 65
Lcup_Dmrt99B 1 YQRTFKCARCRNHGVSALKGKRYCRWRDVCACAKCTLIAERQVMAAQVALRRQAQDEENGSE 65
Lcup_Dmrt93B 1 TNRVFKCARCRNHGMIISLKGHKRCHRFKDCCLVKNCLIAERQVMAAQVALRRQAQDEENGSE 65
Lcup_Dsx 1 PRTPFNCARCRNHLKIALKGHKRYCYVYCNCEKCLTAERQVMAAQVALRRQAQDEENGSE 65
Lful_Dsx 1 ARTPFKCARCRNHLKIALKGHKRYCYVYCNCEKCLTAERQVMAAQVALRRQAQDEENGSE 65
Lmiq_Dsx 1 QRTPFNCARCRNHGYSILKGHKRYCYVYCNCEKCLTAERQVMAAQVALRRQAQDEENGSE 65
Lmod_Dmrt11E 1 MLRTPFKCARCRNHGVSILKGHKRCLRWREDCRCPGCLLVLRQVMAAQVALRRQAQDEENGSE 65
Lmod_Dmrt99B 1 YQRTFKCARCRNHGVSALKGKRYCRWRDVCACAKCTLIAERQVMAAQVALRRQAQDEENGSE 65
Lmod_Dsx 1 PRTPFNCARCRNHLKIALKGHKRYCYVYCNCEKCLTAERQVMAAQVALRRQAQDEENGSE 65
Mext_Dmrt99B 1 YQRTFKCARCRNHGVSALKGKRYCRWRDVCACAKCTLIAERQVMAAQVALRRQAQDEENGSE 65
Mext_Dsx 1 PRTPFNCARCRNHLKIALKGHKRYCYVYCNCEKCLTAERQVMAAQVALRRQAQDEENGSE 65
Mext_Dsx-like 1 NGMNRLCALCRNHLKIPVKGHKRYCYVYCNCEKCLVKEQRVVMHLYFRRQQEEDRGS 65
Mfas_Dsx 1 PRTPFNCARCRNHLKIALKGHKRYCYVYCNCEKCLTAERQVMAAQVALRRQAQDEENGSE 65
Mmac_Dsx 1 NQRHPTCALCRNHQITITLKGHKRYCFFRCTCEKCLTAERQVMAAQVALRRQAQDEENGSE 65
Mmus_Dmrt1 1 SPLRFKCARCRNHGVSPLKGHKRYCFWRDCCQCKNCLIAERQVMAAQVALRRQAQDEENGSE 65
Mrel_Dsx 1 PRTPFNCARCRNHLKIALKGHKRYCYVYCNCEKCLTAERQVMAAQVALRRQAQDEENGSE 65
Mviol_Dsx 1 PRTPFNCARCRNHLKIALKGHKRYCYVYCNCEKCLTAERQVMAAQVALRRQAQDEENGSE 65
Ofur_Dsx 1 PRAPFNCARCRNHLKIALKGHKRYCYVYCNCEKCLTAERQVMAAQVALRRQAQDEENGSE 65
Otau_Dsx 1 PRTPFNCARCRNHLKIALKGHKRYCYVYCNCEKCLTAERQVMAAQVALRRQAQDEENGSE 65
Ppra_Dsx 1 PRTPFNCARCRNHLKIALKGHKRYCYVYCNCEKCLTAERQVMAAQVALRRQAQDEENGSE 65
Psch_Dsx-like 1 NNMNRLCALCRNHLKIPVKGHKRYCYVYCNCEKCLVKEQRVVMHLYFRRQQEEDRGS 65
Smaq_Dmrt99B 1 YQRTFKCARCRNHGVSALKGKRYCRWRDVCACAKCTLIAERQVMAAQVALRRQAQDEENGSE 65
Tcas_Dmrt93B 1 SARVFKCARCRNHGMIISLKGHKRCHRFKDCCLVKNCLIAERQVMAAQVALRRQAQDEENGSE 65
Tcas_Dmrt99B 1 YQRTFKCARCRNHGVSALKGKRYCRWRDVCACAKCTLIAERQVMAAQVALRRQAQDEENGSE 65
Tcas_Dsx 1 PRTPFNCARCRNHLKIALKGHKRYCYVYCNCEKCLTAERQVMAAQVALRRQAQDEENGSE 65
Teri_Dsx-like 1 NMLNRLCALCRNHLKIPVKGHKRYCYVYCNCEKCLVKEQRVVMHLYFRRQQEEDRGS 65
Tdic_Dsx 1 PRTPFNCARCRNHLKIALKGHKRYCYVYCNCEKCLTAERQVMAAQVALRRQAQDEENGSE 65
Tdom_Dmrt99B 1 YQRTFKCARCRNHGVSALKGKRYCRWRDVCACAKCTLIAERQVMAAQVALRRQAQDEENGSE 65
Tdom_Dmrt11E 1 LLRTFKCARCRNHGVSILKGHKRCLRWREDCRCPGCLLVLRQVMAAQVALRRQAQDEENGSE 65
Tdom_Dmrt93B 1 GARRFKCARCRNHGMIISLKGHKRCHRFKDCCLVKNCLIAERQVMAAQVALRRQAQDEENGSE 65
Tdom_Dsx 1 ARTPFKCARCRNHLKIALKGHKRYCYVYCNCEKCLTAERQVMAAQVALRRQAQDEENGSE 65
Tdom_Dsx-like 1 VGRTPSCAQRNHLRVPVGRHKRYCYVYCNCEKCLVKEQRVVMHLYFRRQQEEDRGS 65
Tger_Dsx-like 1 KIPSLRCAQRNHLRVPVGRHKRYCYVYCNCEKCLVKEQRVVMHLYFRRQQEEDRGS 65
Tsub_Dsx 1 QRTPFNCARCRNHGYSILKGHKRYCYVYCNCEKCLTAERQVMAAQVALRRQAQDEENGSE 65
Xant_Dsx 1 PRTPFNCARCRNHLKIALKGHKRYCYVYCNCEKCLTAERQVMAAQVALRRQAQDEENGSE 65
Xlae_Dmrt1 1 SPLRFKCARCRNHGVSPLKGHKRYCFWRDCCQCKNCLIAERQVMAAQVALRRQAQDEENGSE 65
Xlae_Dmrt4 1 YPRTPFKCARCRNHGVSALKGKRYCRWRDVCACAKCTLIAERQVMAAQVALRRQAQDEENGSE 65
Xlae_Dmrt5 1 YPRTPFKCARCRNHGVSALKGKRYCRWRDVCACAKCTLIAERQVMAAQVALRRQAQDEENGSE 65
```

1118 **Figure 1—figure supplement 1.** Multiple sequence alignment of DM domain of  
1119 DMRT family proteins for molecular phylogenetic analysis. The 65 amino acids of 97  
1120 DMRT proteins were used for the molecular phylogenetic analysis.

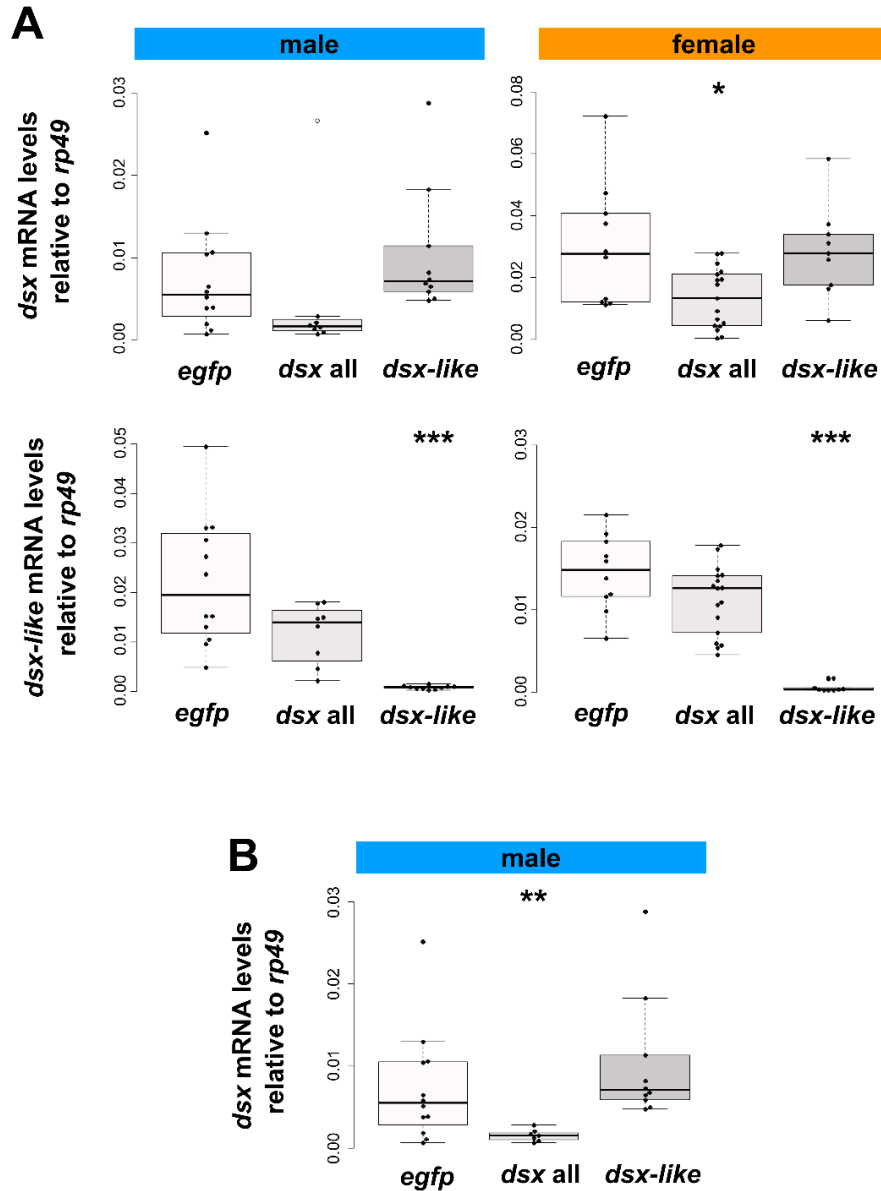
1121



1122

1123 **Figure 1–figure supplement 2.** Comparison of DM domain sequences between Dsx  
 1124 and Dsx-like. The upper figures show the gene structures of *dsx* and *dsx-like*, and the  
 1125 lower one is the result of the multiple sequence alignment of the DM domain in Dsx  
 1126 and Dsx-like of *Thermobia domestica*. The black-highlighted sequences are shared in  
 1127 both proteins.

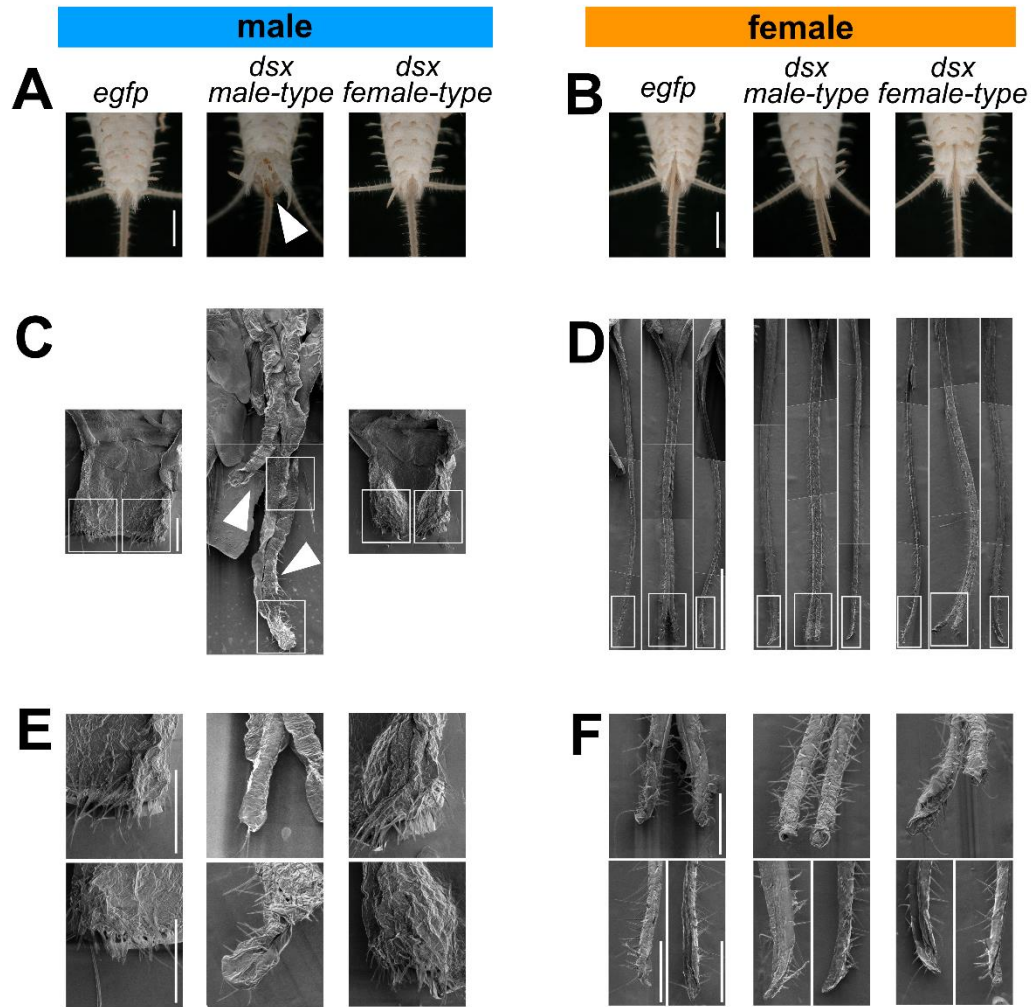
1128



1129 **Figure 1–figure supplement 3.** Expression of *dsx* and *dsx-like* mRNA in nymphal  
 1130 RNAi individuals. (A) results of RT-qPCR assay. The expression profiles of *dsx* and  
 1131 *dsx-like* mRNA were analyzed by RT-qPCR assay and are indicated by their  
 1132 expression level relative to the expression of a reference gene (*ribosomal protein 49*).  
 1133 The upper graphs are the expression of *dsx* mRNA and the lower ones are that of *dsx-*  
 1134 *like* mRNA. The left column is the result in males and the right one is that in females.  
 1135 (B) the expression level of *dsx* mRNA in the nymphal RNAi males after excluding an  
 1136 outlier. To test the outlier, the Smirnov–Grubbs’ test was performed. Results of the  
 1137 Smirnov–Grubbs’ test are shown in Table 3. Results of the Brunner–Munzel test are  
 1138 indicated by asterisks: \* $P < 0.05$ ; \*\* $P < 0.01$ ; \*\*\* $P < 0.001$  and is also described in  
 1139 Table 2.  $P > 0.05$  is not shown. Each plot is an individual. White plot is the outlier.  
 1140 Sample size are listed in Table 2.

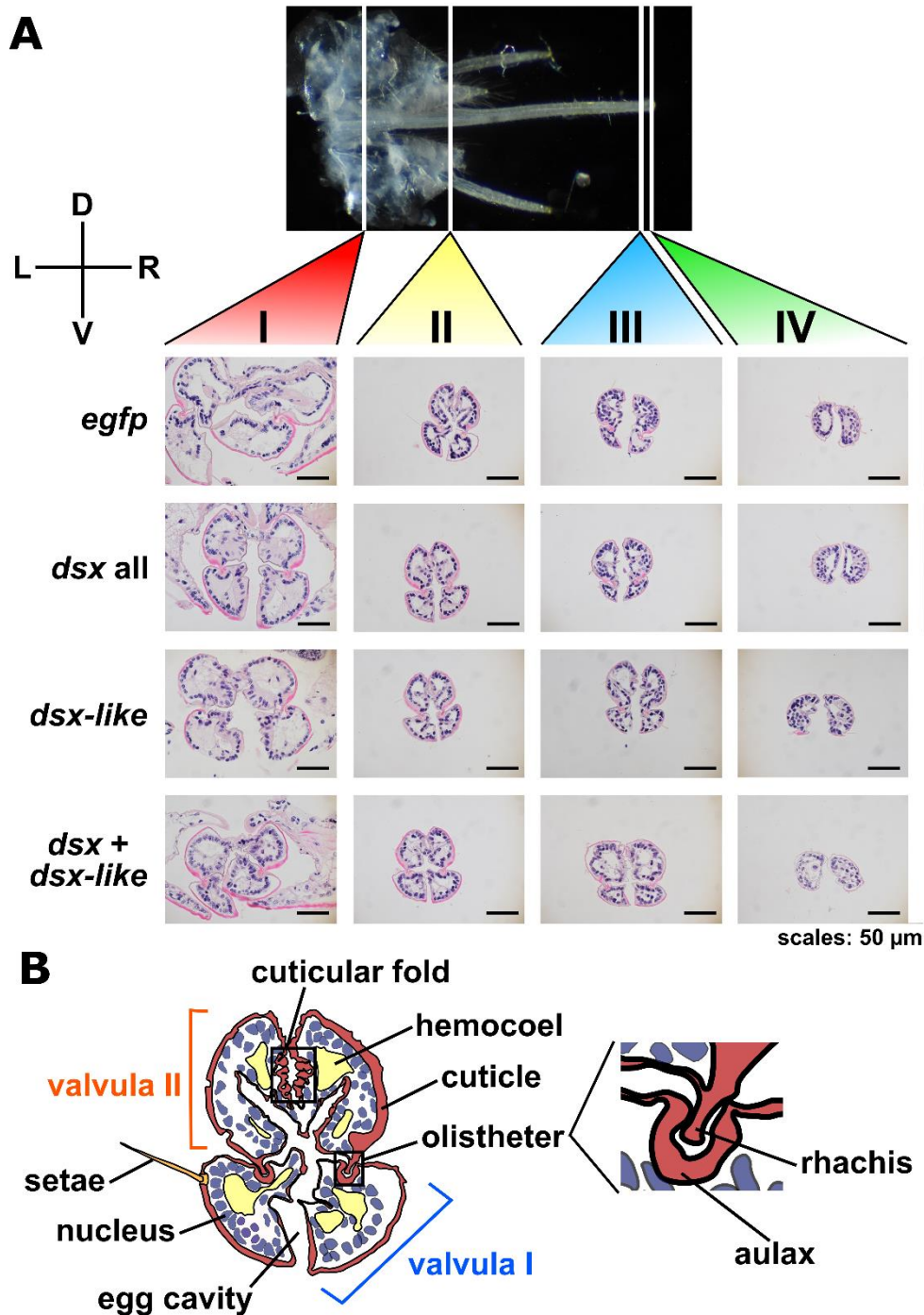
1141



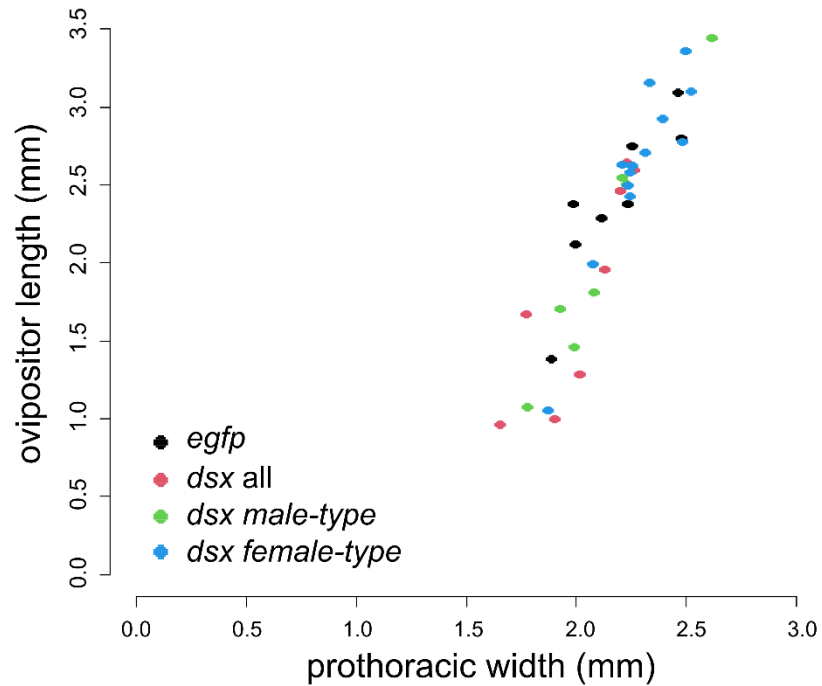


1142 **Figure 2–figure supplement 1.** External genital organs of nymphal RNAi  
 1143 individuals. (A) The penis in ventral view of *dsx* male or female-type RNAi males.  
 1144 (B) The ovipositor in ventral view of *dsx* male or female-type RNAi females. (C)  
 1145 SEM images of the male penis or the ovipositor-like organ. White frames are the areas  
 1146 shown in (E). (D) SEM images of the female ovipositor. Each image is separated into  
 1147 three parts. The left and right image is each lobe of the valvula I. The middle image is  
 1148 the valvula II. White frames are the areas showed in (F). (E) Higher magnification  
 1149 SEM images of the male genital organ in (C). Each image shows the higher  
 1150 magnification view of the area enclosed by the white frame in (C). (F) Higher  
 1151 magnification SEM images of the ovipositor. Each image shows the higher  
 1152 magnification view of the area enclosed by the white frame in (D). The arrowheads  
 1153 show the ovipositor-like organ in the *dsx* male-type RNAi male. Scales: 1000  $\mu$ m (A,  
 1154 B, and D), 100  $\mu$ m (C, E, and F).

1155

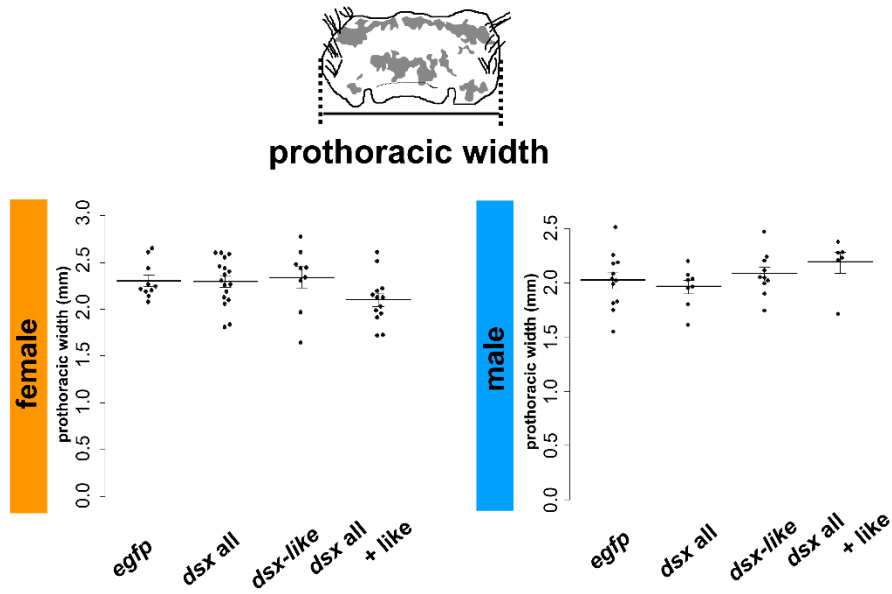


1156 **Figure 2–figure supplement 2.** Morphology of ovipositor in nymphal RNAi  
1157 individuals. (A) Cross-section of the ovipositor. The photos show the morphology of  
1158 the ovipositor in four parts: I (proximal part), II (middle part), III (distal part), and IV  
1159 (most-distal part). D, dorsal; L, left; R, right; V, ventral. Scales: 50  $\mu$ m. (B) Schematic  
1160 figure of the ovipositor morphology. This figure is based on the cross-section of the  
1161 part II in the control female.



1162 **Figure 2–figure supplement 3.** Ovipositor length of *dsx* isoforms RNAi individuals.  
1163 The ovipositor length of *dsx* all, male-, and female-type RNAi females is plotted  
1164 against the prothoracic width. The results of the statistical analysis are described in  
1165 Table 4.

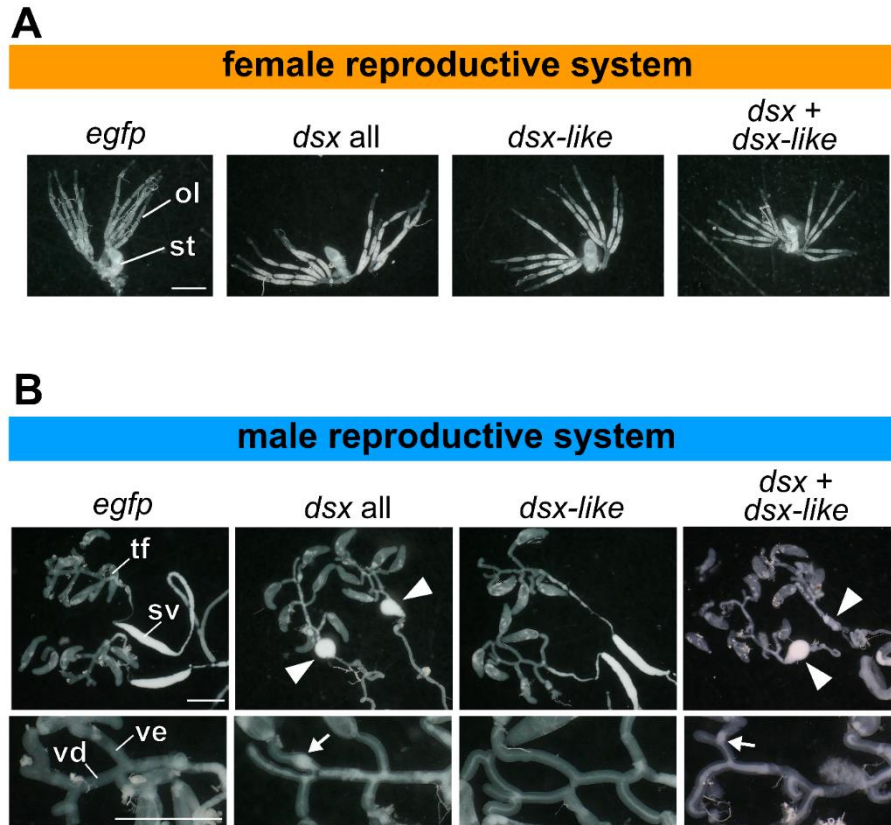
1166



1167

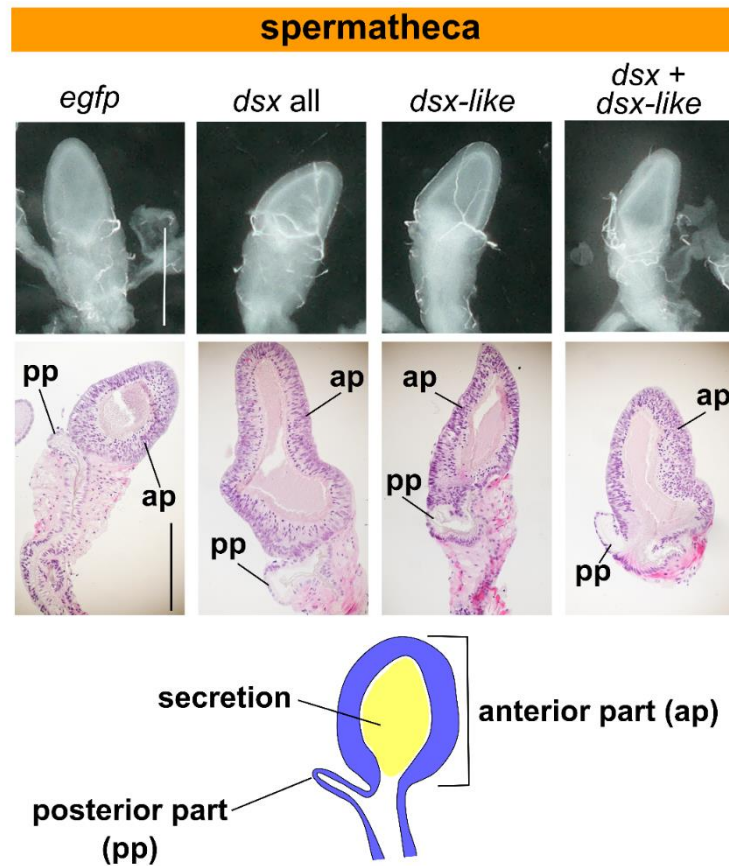
1168 **Figure 2–figure supplement 4.** Prothoracic width of nymphal RNAi individuals. The  
1169 left and right graphs show the female and the male size, respectively. Data shows  
1170 mean  $\pm$  Standard Error (SE). The results of the statistical analysis are described in  
1171 Tables 4 (female) and 5 (male).

1172



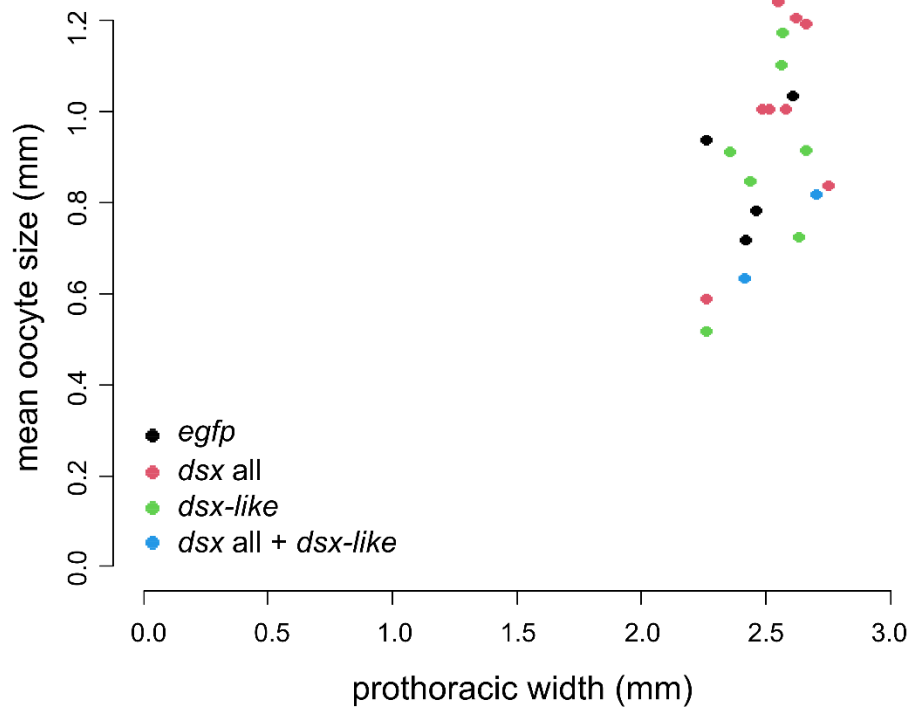
1173 **Figure 3—figure supplement 1. Gonads of nymphal RNAi individuals.** (A) female  
1174 reproductive system. ol, ovariole; st, spermatheca. (B) male reproductive system. The  
1175 upper photos are the are from the testicular follicle to the seminal vesicle. The lower  
1176 ones are the high-magnification image of the vas efferens and the vas deferens. The  
1177 arrowheads show the round-shape seminal vesicle. The arrows indicate sperm clots in  
1178 the vas efferens. sv, seminal vesicle; tf, testicular follicle; ve, vas efferens; vd, vas  
1179 deferens. Scales: 1 mm.

1180



1181 **Figure 3–figure supplement 2.** Morphology of spermatheca in nymphal RNAi  
1182 individuals. The upper photos show the light microscopic images of the spermatheca.  
1183 The middle ones are paraffin sections of the spermatheca. The lower one is the  
1184 schematic image of the spermatheca of *T. domestica*. Scales: 500  $\mu$ m.

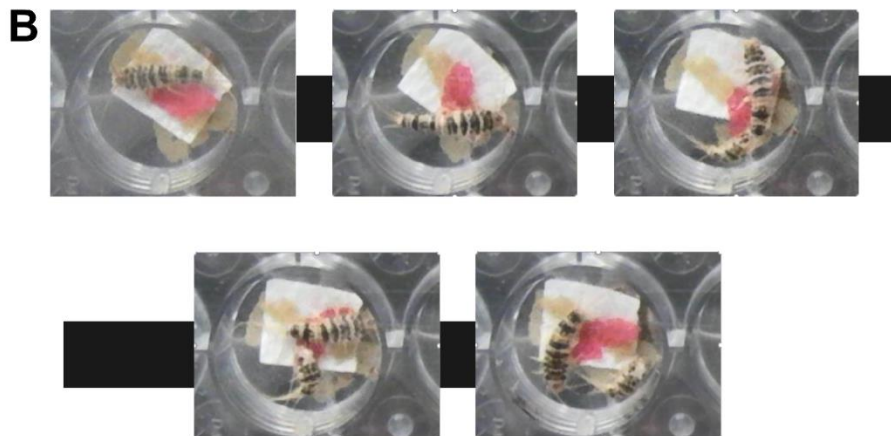
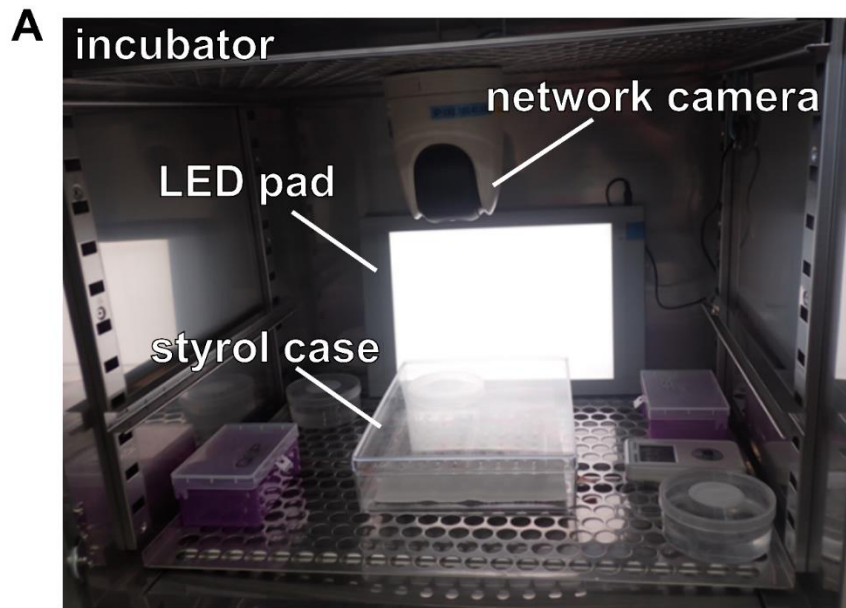
1185



1186

1187 **Figure 3—figure supplement 3.** Oocyte size of *dsx* isoforms RNAi individuals. The  
1188 oocyte size of *dsx all*, *dsx-like*, and both *dsx* and *dsx-like* RNAi females is plotted  
1189 against the prothoracic width. The results of the statistical analysis are described in  
1190 Table 4.

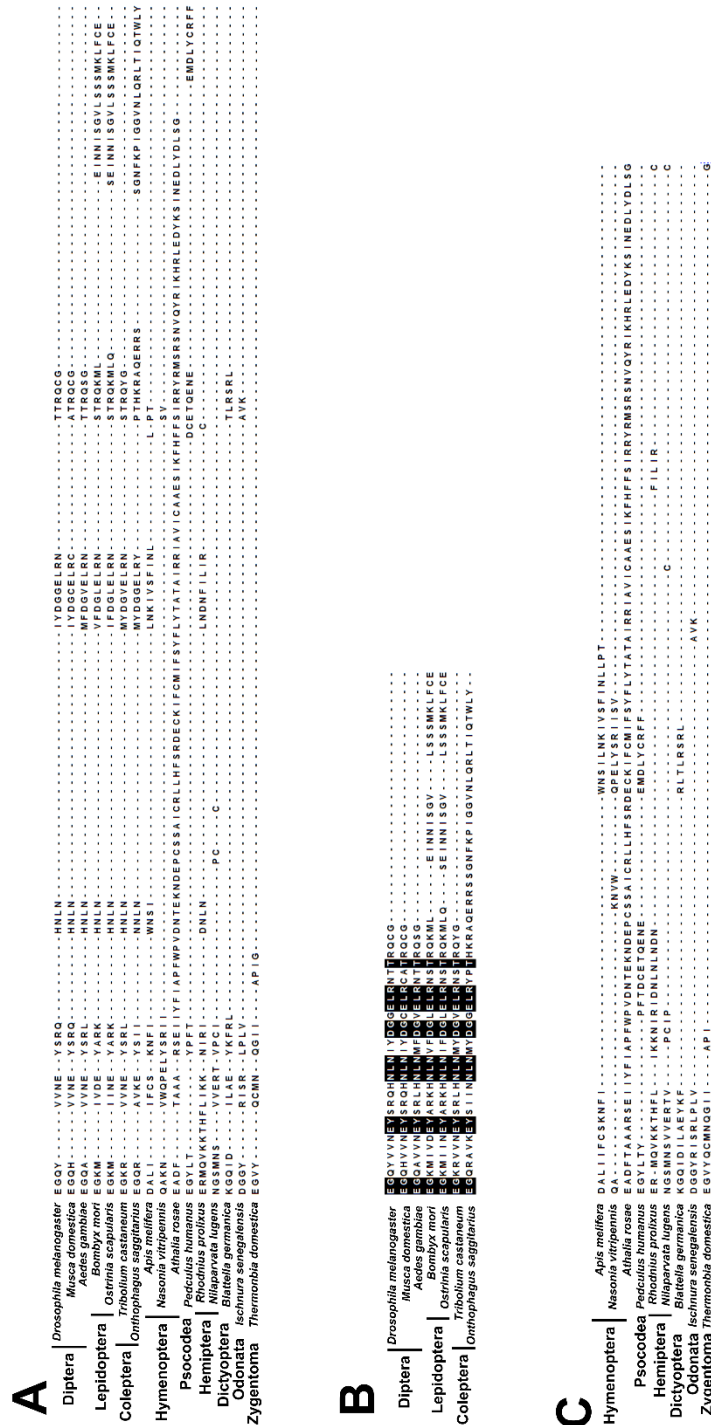
1191



1192 **Figure 4—figure supplement 1.** Time-lapse imaging system. (A) A photo of the time-  
1193 lapse imaging system used to observe the molt of *T. domestica*. (B) The images  
1194 during the molt.

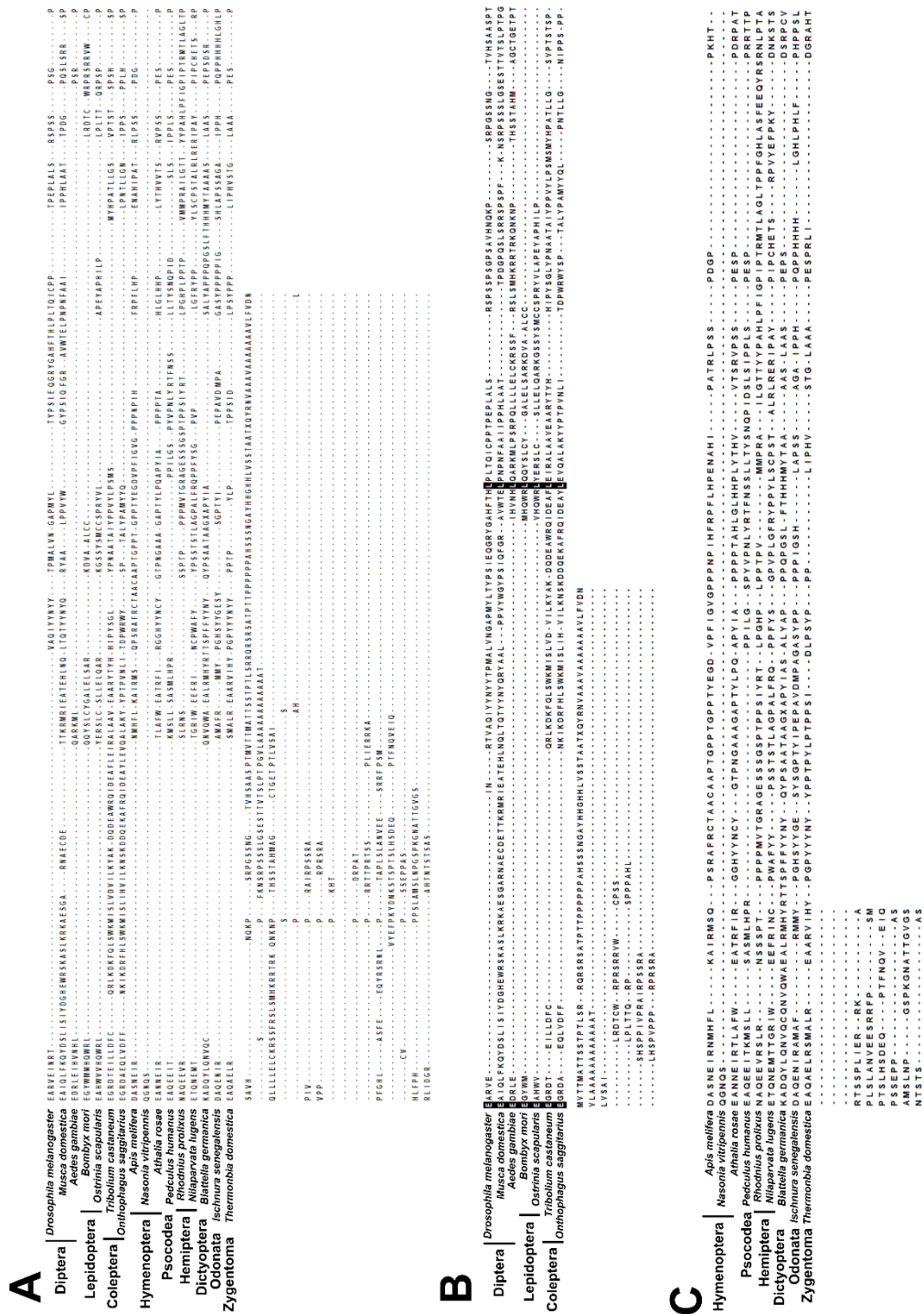
1195





1196 **Figure 5–figure supplement 1.** Multiple sequence alignments of insect Dsx female-  
 1197 specific region. (A) Comparison of the female-specific region of insect Dsx among  
 1198 the all taxa. (B) Comparison of the female-specific region of insect Dsx among the  
 1199 taxa with the dual-functionality. (C) Comparison of the female-specific region of  
 1200 insect Dsx among the taxa with the single-functionality. The black-highlighted  
 1201 sequences are shared in all given taxa.

1202



1203 **Figure 5–figure supplement 2.** Multiple sequence alignments of insect Dsx male-  
 1204 specific region. (A) Comparison of the male-specific region of insect Dsx among the  
 1205 all taxa. (B) Comparison of the male-specific region of insect Dsx among the taxa  
 1206 with the dual-functionality. (C) Comparison of the male-specific region of insect Dsx  
 1207 among the taxa with the single-functionality. The black-highlighted sequences are  
 1208 shared in all given taxa.

1209

1210